

Northumbria Research Link

Citation: Mehmood, Imran, Li, Heng, Umer, Waleed, Arsalan, Aamir, Saad Shakeel, M. and Anwer, Shahnawaz (2022) Validity of facial features' geometric measurements for real-time assessment of mental fatigue in construction equipment operators. *Advanced Engineering Informatics*, 54. p. 101777. ISSN 1474-0346

Published by: Elsevier

URL: <https://doi.org/10.1016/j.aei.2022.101777>
<<https://doi.org/10.1016/j.aei.2022.101777>>

This version was downloaded from Northumbria Research Link:
<https://nrl.northumbria.ac.uk/id/eprint/50990/>

Northumbria University has developed Northumbria Research Link (NRL) to enable users to access the University's research output. Copyright © and moral rights for items on NRL are retained by the individual author(s) and/or other copyright owners. Single copies of full items can be reproduced, displayed or performed, and given to third parties in any format or medium for personal research or study, educational, or not-for-profit purposes without prior permission or charge, provided the authors, title and full bibliographic details are given, as well as a hyperlink and/or URL to the original metadata page. The content must not be changed in any way. Full items must not be sold commercially in any format or medium without formal permission of the copyright holder. The full policy is available online: <http://nrl.northumbria.ac.uk/policies.html>

This document may differ from the final, published version of the research and has been made available online in accordance with publisher policies. To read and/or cite from the published version of the research, please visit the publisher's website (a subscription may be required.)

20 Kong SAR

21 **Corresponding Author ****

22 Waleed Umer, Ph.D., (Email; waleed.umer@northumbria.ac.uk)

23 Department of Mechanical and Construction Engineering, Northumbria University, Newcastle upon Tyne NE7

24 7YT, United Kingdom

25

26

27

28

29

30

31

32

33

34

35

36

37

38

39 **Abstract**

40 Operating construction equipment for extended periods of time may lead to mental fatigue and, as a result, an
41 increased risk of human error-related accidents and jeopardized health problems for the operators. Therefore, to
42 limit the risk of accidents and protect operators' wellbeing, their mental fatigue must be monitored reliably and in
43 real time. Recently, many invasive technologies have been employed to alleviate this problem, but they entail the
44 wearing of physical sensors, which may instigate irritation and discomfort. This study proposes a non-invasive
45 mental fatigue monitoring method using geometric measurements of their facial features that does not require the
46 operators to wear sensors on their body. The study further validates the proposed method by comparing it with
47 wearable [electroencephalography](#) (EEG) technology to establish its ecological validity for construction equipment
48 operators. To serve the purpose, a one-hour excavator operation by sixteen construction equipment operators was
49 conducted on a construction site. Ground truth, brain activity using wearable EEG, and geometric measurements
50 of facial features were extracted and analyzed at the baseline and every 20 min for one hour. A considerable
51 temporal variation was found in the reported metrics (eye aspect ratio, eye distance, mouth aspect ratio, face area,
52 and head motion) and were significantly correlated with ground truth and EEG metric. Furthermore, the brain
53 visualization pattern obtained from EEG was also associated with the variations in the facial features. The findings
54 of the study reveal that construction equipment operators' mental fatigue can be monitored non-invasively using
55 geometrical measurements of facial features.

56 Keywords: mental fatigue, construction equipment operators, construction safety, facial features,
57 [electroencephalography](#)

58 1 Introduction

59 The construction industry has reputation for its poor safety performance (Ke et al., 2021b). Despite huge positive
60 impacts, the safety of the workforce in the construction industry is the most neglected and unresolved challenge.
61 Globally, the construction industry has an excessively high accident rate (ILO, 2022). More specifically, about
62 20% of fatal accidents in the United States and 40% of fatal accidents in Singapore happen in the construction
63 industry (Feng et al., 2015, OSHA, 2019). Similarly, the Hong Kong construction industry also reported 2947 and
64 2532 accidents in 2019 and 2020, respectively. In addition, statistics for the first three months of 2022 reveal that
65 the construction industry in Hong Kong recorded the highest number of fatalities and accident rate among all other
66 industrial sectors (Labor, 2022). Moreover, construction has been listed as the second most accident-prone industry
67 in Pakistan relative to other industries, and the percentage of accidents has increased significantly over the past
68 several years. For instance, 16.27%, 17.27%, and 19.70% in 2014-15, 2017-18, and 2020-21, respectively (PBS,
69 2015, PBS, 2018, PBS, 2021). Besides, safety remains a key concern in the Chinese construction industry, as it
70 accounted for over a third of all recorded incidents (CLB, 2020). Additionally, the People's Republic of China's
71 Ministry of Emergency Management reported in 2018 that the total number of accidents had increased year-on-
72 year and has remained high. Furthermore, the accident and death rates increased by 7.8 percent in the first half of
73 2018 to 1,732 accidents and 1.4 percent to 1,752 deaths, respectively (MEM, 2018). Among the overall
74 construction accidents, equipment accounted for one fifth of the total accidents (Labor, 2016). Likewise, OSHA
75 also found that struck-by accidents are among the four major causes of fatalities in the construction industry.
76 Construction equipment is used in the construction industry to perform different complex tasks such as excavation,

77 lifting materials, compaction, etc. Such tasks are mentally demanding and require the equipment operators to
78 maintain a certain level of sustained attention and vigilance (Li et al., 2020b). Wagstaff and Sigstad Lie (2011)
79 stated that such prolonged construction operations and vigilant tasks induce mental fatigue among construction
80 equipment operators. When an operator is subjected to mental fatigue, he is unable to continue equipment
81 operations due to prolonged attention. It hampers the equipment operators' judgement and concentration (Das et
82 al., 2020). They undergo a decrease in productivity and performance (Masullo et al., 2020). This makes equipment
83 operators more vulnerable to equipment-related accidents and, subsequently, causes workplace injuries and
84 fatalities. Therefore, prevention of construction equipment operators' attention failure plays an important role in
85 enhancing site safety (Han et al., 2019). Therefore, it is crucial that the mental fatigue of construction equipment
86 operators be automatically monitored so that safety personnel can intervene immediately if necessary.

87 Safety is a fundamental need for anyone participating in construction work. Therefore, for construction safety,
88 many studies have attempted to assess the mental fatigue of construction equipment operators. Initially, mental
89 fatigue was assessed by relying on the subjective assessment of operators (Turner and Lingard, 2020). Among
90 them, the most widely utilized subjective assessment tool is NASA-TLX (Hart, 2006). As such, this assessment
91 was not suitable for continuous monitoring of mental fatigue since it hampers the routine work of operators, it is
92 intrusive in nature, time-consuming, and is based on biased self-reporting of workers; hence, it lacks accuracy
93 (Umer et al., 2020, Han et al., 2019). Over the past few decades, advances in technology have made it possible to
94 develop devices that provide objective assessments of mental fatigue. Therefore, the researchers were motivated
95 to perform a more objective and real-time assessment of mental fatigue using physiological measurements such as

96 electroencephalogram (Jeon and Cai, 2022, Ke et al., 2021a, Wang et al., 2019), electrodermal activity (Umer,
97 2022, Lee et al., 2021, Choi et al., 2019), eye tracking (Noghabaei et al., 2021, Li et al., 2020b, Han et al., 2020)
98 and electrocardiograph (Umer et al., 2022, Zhao et al., 2012). As a result of the fact that when a person's mental
99 state changes, so do the values and parameters of physiological signals and their accompanying parameters (Dziuda
100 et al., 2021). Even though these technologies have shown promising results in the diagnosis of mental fatigue,
101 there are several issues with their use. The equipment operators must wear these devices on their bodies making
102 them invasive in nature and at the same time causing annoyance while performing equipment operations (Li et al.,
103 2020b). These techniques are based on the electrical conductivity of the operator's body, and electrical signals are
104 susceptible to harsh construction site conditions. The application of these technologies sometimes requires skin
105 preparation for sensors and also necessitates limited physical activity to minimize artifacts (Chen et al., 2015).
106 Some of these technologies, including electroencephalography, have poor spatial resolution (Kaur et al., 2022).
107 Due to the fact that electrodes assess surface activity, it is unknown whether the signals originate near the surface
108 or deep within the brain region. Also, most of the studies were conducted in simulated scenarios, such as by Liu
109 et al. (2021) and Li et al. (2019b), which limits their applicability and reliability for construction sites and
110 equipment operators. This significantly limits their occupational use for detection of fatigue (Shi et al., 2017).
111 Thus, there exists a knowledge gap to automatically detect the operators' mental fatigue by non-invasive and
112 contact-free measurements without disrupting their ongoing equipment operations. Likewise, a low-cost,
113 automated early warning system for the mental fatigue of construction equipment operators will help to make
114 construction sites safer for operations.

115 Accordingly, this study proposes geometrical measurements of construction equipment operators' facial features
116 as a manifestation of mental fatigue through non-invasive and contact-free measurements. As per the study by Ma
117 et al. (2021), the human face not only shows direct personal information but also shows indirect emotions. Dziuda
118 et al. (2021) reported that the continuous analysis of face images of drivers acquired while driving allows effective
119 and contactless detection of fatigue. Similarly, Cheng et al. (2019) concluded that observing a person's facial
120 expressions and indications can reveal clues to their level of stress and fatigue. Earlier studies also indicate the
121 usefulness of facial features for fatigue detection. At the beginning of the 1990s, the percentage of time that the
122 eyes were 80% to 100% closed was adopted to research fatigue in drivers (Daza et al., 2014, Zhang and Zhang,
123 2010). Later ranges of 70% to 100% (Lin et al., 2015) and 75% to 100% (Henni et al., 2018) of eye closure were
124 considered in other studies. Other indicators of mental fatigue were also proposed. The most measurable indicator
125 related to eyes were eye aspect ratio (Kuwahara et al., 2022, El Kerdawy et al., 2020), blinking rate (Bachurina
126 and Arsalidou, 2022, Zargari Marandi et al., 2018); and eye distance (Giannakakis et al., 2017). Similarly, Wang
127 et al. (2018) reported that as much as 80% of the information our brains get originates from our eyes. Eye behavior
128 can therefore be utilized to evaluate our mental state. Additionally, Chew et al. (2021) analyzed gaze behavior
129 patterns to assess the perceived workload. Nevertheless, eye blinks are also considered in the latest literature on
130 driver fatigue research (Aravind et al., 2019). Similarly, Li et al. (2021) used self-report, eye blinking rate, and R-
131 value as indicators to substantiate the driver's fatigue state. Additional information regarding the mental fatigue
132 can also be obtained by tracking the position of the driver's head. It has been reported that under stressful
133 conditions, head motions are more frequent and quicker, with a greater overall amount of head motion (Ansari et

134 al., 2022, Giannakakis et al., 2018). Furthermore, research shows that fatigued situations have been demonstrated
135 to have an impact on mouth-related features such as lip movement (Iwasaki and Noguchi, 2016). Similarly,
136 Giannakakis et al. (2017) reported increased mouth activity during stressful situations.

137 Despite the potential of automated facial features for the mental fatigue assessment of construction equipment
138 operators, there is a scarcity of research using geometric measurements of facial features to understand equipment
139 operators' mental fatigue on real construction sites. Additionally, it is challenging to use findings from other
140 occupations, such as drivers, for fatigue monitoring in excavator operators due to the substantial differences
141 between the work patterns of drivers and excavator operators. For example, during equipment operations,
142 excavator operators move their heads continuously to track the excavator's bucket (Liu et al., 2021). Therefore, it
143 remains unknown whether geometric measurements of facial traits under such circumstances can still be used to
144 detect construction equipment operators' mental fatigue. Thus, the ecological validity of the geometric measures
145 of facial features for mental fatigue monitoring of construction operators is still questionable. Consequently, a
146 research gap exists for the development and testing of an objective, automatic, and non-invasive method for
147 assessing operators' mental fatigue. To fill this gap, firstly, the study proposes a non-invasive assessment of
148 temporal geometric measurements of facial features to detect mental fatigue. Secondly, the study compares
149 geometric measurements to wearable electroencephalography measurements, which is an established invasive
150 method for mental fatigue assessment of construction workers. Many researchers have utilized it extensively to
151 monitor the mental fatigue and stress of construction workers, for instance studies by Lee and Lee (2022), Wang
152 et al. (2022), Jeon and Cai (2022), Ke et al. (2021a), Xing et al. (2020b), Li et al. (2019a), Wang et al. (2019),

153 Jebelli et al. (2019), Jebelli et al. (2018a), Hwang et al. (2018), and Wang et al. (2017). This comparison serves to
154 ecologically validate the geometric measurement of facial features in terms of their applicability to construction
155 equipment operators' as well as their effective use during routine operations by operators without interfering with
156 their on-site operations. As a result, the proposed study is expected to improve the current assessment of mental
157 fatigue in a non-invasive way through contact-free measurements.

158 **2 Methodology**

159 The overview of the research process and experiment procedure is depicted in Figure 1 and Figure 2, respectively.
160 It shows the proposed approach for identifying mental fatigue in construction equipment operators by using
161 geometric measurements of facial features collected through video recordings. An excavator operating experiment
162 was conducted at a construction site to collect related data for detecting the mental fatigue of construction
163 equipment operators. On different days, the experiment was conducted at the same time, i.e., from 9:00am to
164 11:00am (Li et al., 2019b, Zhao et al., 2012) in the morning under similar weather conditions, i.e., clear weather
165 on all data collection days. The experiment was based on a monotonous and prolonged excavating and discharge
166 task on a construction site. All the excavator operators were directed to complete a monotonous and prolonged
167 excavation task for an hour, which included ground excavation and moving the material from pits to transport
168 vehicles. Mental fatigue was induced using the time-on-task procedure. Simultaneously with their tasks, the
169 operators were video recorded to collect data on their facial features via a mobile camera. Besides, the NASA-
170 TLX score was utilized to quantify the subjective assessment of equipment operators' mental workload. The
171 subjective mental fatigue levels were assessed at the start as a baseline measurement and every 20 min for the one-

172 hour experiment (i.e., at 20, 40, and 60 min). Geometric measurements of facial features were then extracted from
 173 each frame, and artifacts were removed using a normalization coefficient Q . It is a Euclidean distance along the
 174 nose line. Apart from visual cues, EEG data for each equipment operator was also collected for every experiment
 175 phase. For the purpose of statistical analysis, since the subjective mental fatigue levels were assessed at baseline
 176 and every 20-min experiment phase, the continuous real-time data of facial features from video frames and EEG
 177 sensor data was averaged for the respective time points (i.e., at 20, 40, and 60 min), as shown in block-B of Figure
 178 1. Mental fatigue was detected by evaluating temporal changes in facial features and through EEG sensors between
 179 the time points. Finally, the detected mental fatigue with EEG and geometric measurements of facial features were
 180 correlated to develop ecological validity for construction equipment operators.

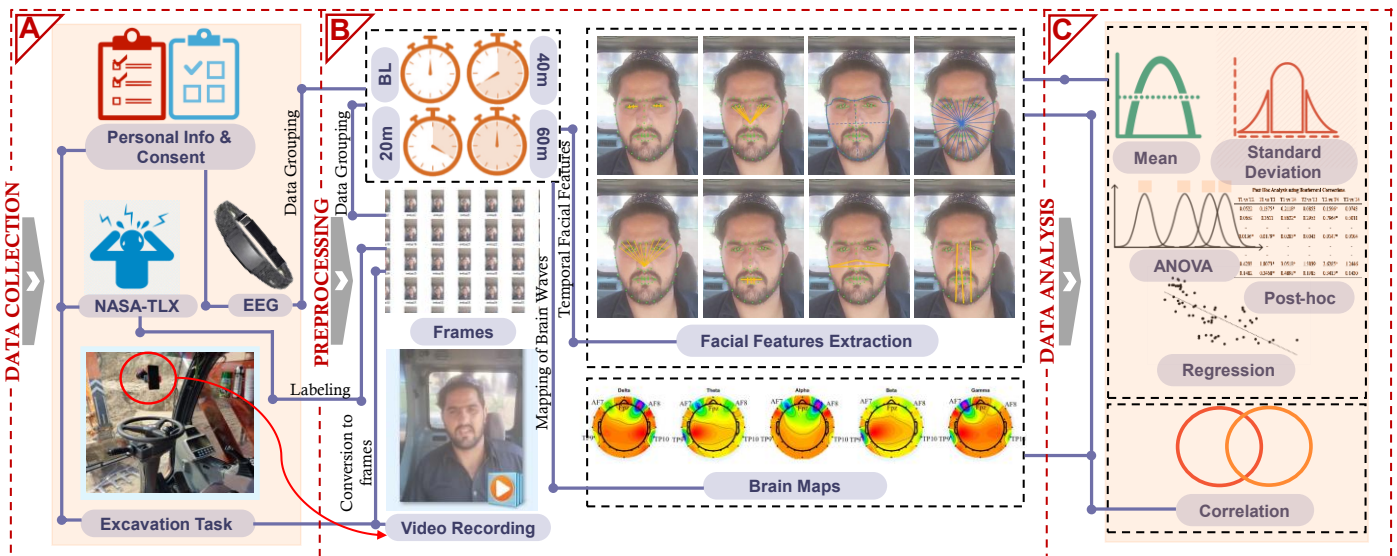


Figure 1: Overview of the research process

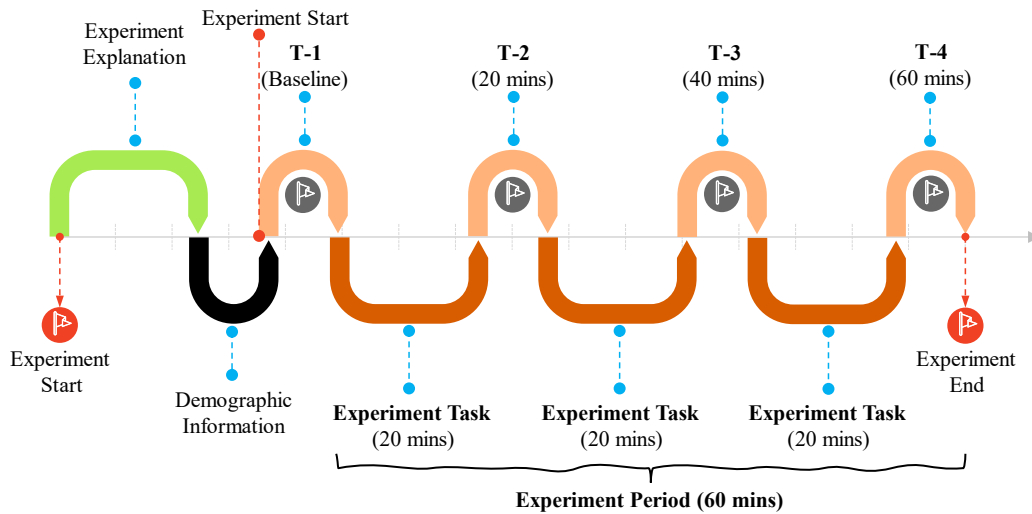


Figure 2: Experiment procedure; T1, T2, T3 and T4 represents the phases for assessments through NASA-TLX, facial features and EEG

182 **2.1 Participants**

183 Sixteen construction equipment operators with a mean age of 32.63 years (SD = 4.11) were included in the on-
 184 field data collection. We determined the sample size of excavator operators to recruit for our research investigations
 185 based on sample sizes from previous studies. In earlier studies with similar purposes, 12 excavator operators (Li
 186 et al., 2019b), 12 crane operators (Das et al., 2020), 11 drivers (Ahn et al., 2016), 6 excavator operators (Li et al.,
 187 2020b), and 5 crane operators (Liu et al., 2021) were recruited. Considering previous research in the literature, we
 188 decided that more than fifteen operators would be sufficient for our investigation and to justify our results. In
 189 addition, the results showed statistically significant differences, demonstrating that the sample size was adequate
 190 to infer valid conclusions. Furthermore, all the excavator operators who participated in the study were male. All
 191 the equipment operators were excavator operators, with prior experience of excavation operations at construction
 192 sites. The excavator operators indicated in their self-report that they were well rested and in good health. All the
 193 excavator operators reported having slept at least eight hours during the previous night and abstained from

194 alcoholic drinks for 24 hours before experimentation. On their assigned day, the operators were to report directly
195 to the experiments and perform no other duties or activities prior to the commencement of the experiment. The
196 recruited excavation operators had normal vision and provided informed consent before the data collection. The
197 study was approved by the ethics subcommittee of the Hong Kong Polytechnic University (Reference Number:
198 HSEARS20210927008) and conducted in accordance with the Declaration of Helsinki. Table 1 provides the
199 demographic information of the excavation operators.

200 **Table 1: Construction equipment operators' demographic information**

	Mean	SD	Range (Min-Max)
Age (Years)	32.63	4.11	13 (26-39)
Job Experience (Years)	7.44	2.90	9 (2-11)
Height (cm)	174.50	5.06	18 (166-184)
Weight (kg)	77.31	5.99	23 (68-91)
Body Mass Index (kg/m ²)	25.43	2.29	8.30 (21.46-29.76)

201 2.2 **Equipment and Measurement**

202 2.2.1 *Subjective assessment scales*

203 The NASA-TLX score was used for the labeling of construction equipment operators by assessing their individual
204 subjective feelings of mental fatigue. The NASA-TLX score was utilized to quantify equipment operators' mental
205 workload. It has been widely used in various research investigations since its development, and its reliability and
206 sensitivity have been tested in a consistent number of independent tests (Hart, 2006). Likewise, studies by Liu et
207 al. (2016) and Puspawardhani et al. (2016) also stated that NASA-TLX is a popular component of research studies
208 since it is reliable and easy to use. Furthermore, temporal increase in NASA-TLX scores for the same task is
209 considered as a subjective indicator of mental fatigue (Li et al., 2020b). The subjective assessment was used as a

210 ground truth for construction equipment operators' mental fatigue levels and was used to compare temporal
211 outcomes of facial features' geometric measurements.

212 *2.2.2 Camera-based video recording*

213 A color video camera was mounted on the inner side of the excavator to film the operators while they sat in the
214 cabin. The approximate distance between the operator and the camera was 0.6m. The camera was installed on the
215 windscreen of the equipment in such a manner that the operator's usual work was not disrupted by its presence.
216 The sampling frequency of the color video camera was 30 frames per second (24-bit RGB with three channels or
217 8-bit RGB per channel), with a resolution of 1440 x 1440 pixels. Furthermore, unlike other industries where the
218 working conditions are stable, construction is a dynamic and complex industry with distinct working
219 circumstances (Xing et al., 2020a). In this case, variations in illumination or non-uniform lighting
220 conditions can impair facial detection performance. As discussed in the manuscript, the performance of
221 our method depends heavily on the accurate localization of facial landmarks, which are hard to detect in
222 low-light environments. Furthermore, we collected data from the real construction site at the same time
223 on separate days while keeping weather forecasts in mind to avoid the extreme impacts of illumination.
224 As a result, the overall effect of illumination and temperature was comparable for all operators.
225 Furthermore, on days during data collection, the average minimum and maximum temperatures were
226 29.1°C and 30.4°C, respectively. Additionally, on all days, the weather was clear.

227 *2.2.3 Electroencephalogram (EEG) Recording*

228 We used the Muse headband, which is a flexible and easy-to-use EEG recording system, to acquire EEG signals.

229 It is a headband with four channels and dry electrodes at AF7, AF8, TP9, and TP10. FPz, being the reference
230 electrode, is placed at the forehead position. The material used for the electrodes is silver. The Muse headband
231 records EEG data at a sampling rate of 256 Hz. The Muse headband was linked to a smart phone through Bluetooth
232 so that data could be transmitted. Using an app called "Mind Monitor," EEG data was recorded on a smart phone
233 and then sent to a PC to be processed later (Arsalan et al., 2019).

234 2.3 Data Preprocessing

235 2.3.1 Data Labeling and Facial Feature Extraction

236 All the operators were video recorded for one hour while performing excavation operations at the construction site.
237 Initially, each operator's captured video was transformed into frames using OpenCV (an open-source computer
238 vision library in Python). This resulted in 108,000 frames for each operator during the whole experiment since the
239 frequency of the camera was 30 frames per second. Subsequently, these frames for each operator were divided into
240 four groups as per the experiment phases, i.e., baseline, 20, 40, and 60 min for further analysis. The frames were
241 then denoted as $F_{o,p}$ where o is the excavation operator, p represents each experiment phase and expressed as
242 vector, $p \in \{ET_1, ET_2, ET_3, ET_4\}$, 1 for baseline, 2 for data at 20 min, 3 for data at 40 min and 4 for data at
243 60 min. Hence, the pre-processing resulted in 16 segments of frames for each experiment phase, owing to the
244 number of operators being 16 and each operator's data being divided into four groups. Thus, the total number of
245 frames processed was 1,728,000. Following the successful division of frames into experiment phases, the next
246 stage was to recognize the faces in each frame and extract the respective facial features for further analysis. The
247 facial detection process was performed on each frame from the video recording using a local constrained neural

248 field model (Baltrušaitis et al., 2016). This model was applied to detect the operators' face in each frame and
 249 produced a vector L of 68 landmarks identified on the operators' face in every frame using Dlib (King, 2009) and
 250 expressed as a vector $L = [q_1, q_2, q_3, \dots, q_i]^T$. Where q_i is a detected face landmark in any frame with
 251 coordinates (a_i, b_i) , T is the number of any frame, and i is index of detected landmarks in any frame, i.e.,
 252 between 1 to 68. Eq. 1 was then used to compute the Euclidean distance between any two landmarks. This
 253 Euclidean distance was eventually used to determine the geometric measurement of eight facial features, as in the
 254 previous studies conducted by Cech and Soukupova (2016) and Bevilacqua et al. (2018). The proposed eight facial
 255 features were computed separately from each individual frame, and the details of the eight facial features have
 256 been listed in Table 2 and shown in Figure 3.

257 **Table 2: Details of extracted facial features**

Feature	Equation
<u>Eye Aspect Ratio (EAR)</u> : Ratio of height and width of an eye	$EAR = \frac{\ p_{42} - p_{38}\ + \ p_{41} - p_{39}\ }{2\ p_{40} - p_{37}\ }$
<u>Eye Distance (ED)</u> : Sum of the distance between anchor and eye landmarks.	$ED = \ p_{37} - p_{31}\ + \ p_{38} - p_{31}\ + \ p_{39} - p_{31}\ + \ p_{40} - p_{31}\ + \ p_{41} - p_{31}\ + \ p_{42} - p_{31}\ $
<u>Eyebrow Distance (EBD)</u> : Sum of the distance between anchor and eyebrow landmarks.	$EBD = \ p_{23} - p_{31}\ + \ p_{24} - p_{31}\ + \ p_{25} - p_{31}\ + \ p_{26} - p_{31}\ + \ p_{27} - p_{31}\ $
<u>Mouth Aspect Ratio (MAR)</u> : Ratio of height and width of mouth	$MAR = \frac{\ p_{68} - p_{62}\ + \ p_{67} - p_{63}\ + \ p_{66} - p_{64}\ }{3\ p_{55} - p_{49}\ }$
<u>Nose to Jaw Ratio (NJR)</u> : Distance between anchor landmark and jaws	$NJR = \frac{\ p_{31} - p_3\ }{\ p_{15} - p_3\ }$
<u>Nose to Chin Ratio (NCR)</u> : Distance between anchor landmark and chin	$NCR = \frac{2\ p_{31} - p_9\ }{\ p_{22} - p_8\ - \ p_{23} - p_{10}\ }$

Face Area (FA): Area of a closed polygon formed by joining the external landmarks on the face

$$FA = \frac{1}{Q} \sum_{i=1}^{N=27} (S(S - d(p_1, p_{31}))^2 (S - d(p_2, p_{31}))^2 (S - d(p_1, p_2))^2),$$

$$\therefore S = \frac{d(p_1, p_{31}) + d(p_2, p_{31}) + d(p_1, p_2)}{2}$$

Head Motion (HM): Sum of the distance between anchor to external landmarks of face, per frame

$$H_{mot} = \frac{1}{Q} \sum_{i=1}^A |p_a - p_b|$$

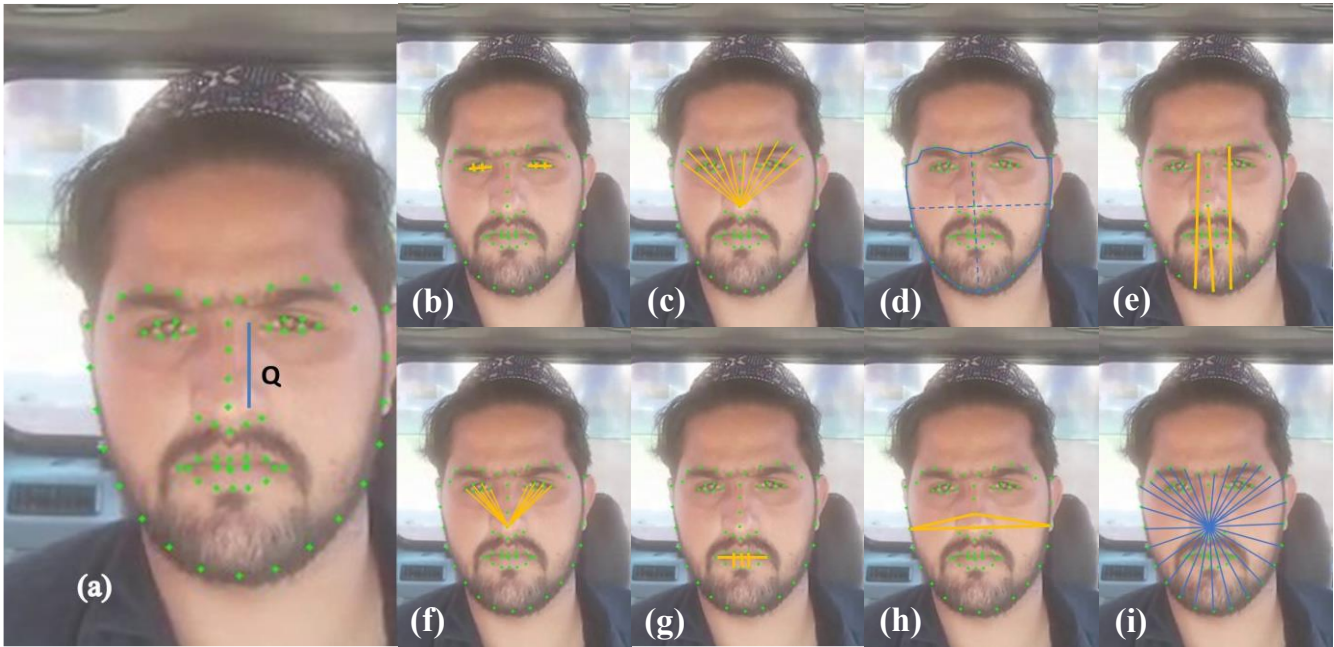


Figure 3: Extraction of facial features; (a) 68 landmarks detection, (b) eye aspect ratio, (c) eyebrows (d) face area (e) nose-to-chin ratio (f) eye distance (g) mouth aspect ratio (h) nose-to-jaw ratio (i) head motion

258 2.3.2 Artifacts Removal

259 The data collected even in the experimental setting contains artifacts, which are undesired variations in the
 260 collected data due to external sources (Sweeney et al., 2012). These artifacts need to be removed since their
 261 existence within the data may easily misinterpret it and create skewness in analysis (Jebelli et al., 2018b, Hwang
 262 et al., 2018). In the case of excavator operators, they undergo continuous excessive and extreme movements during
 263 ongoing excavation operations. These movements are due to equipment vibrations as well as the movements of

264 operators when tracking bucket to excavate and dump the earth. Such movements cause artifacts that need to be
265 removed from the collected data. In the case of facial recognition and facial feature extraction, the facial regions
266 having stable values are used for artifact removal. As reported in the research by Bevilacqua et al. (2018) and
267 Giannakakis et al. (2017), the length of the nose line formed by joining the nose landmarks expressed by vector
268 $Q = [q_{28}, \dots, q_{32}]^T$ was used to remove artifacts, shown in Figure 3(a). Firstly, the landmarks shown by the
269 vector Q were used to calculate the Euclidean distance (expressed as Eq 1) of the nose line. After that, all the
270 facial features were then divided by Q to get normalized facial features from each frame.

271
$$d(q_1, q_2) = \sqrt{(a_2 - a_1)^2 + (b_2 - b_1)^2} \quad Eq. 1$$

272 The recorded EEG signals are subjected to artifact removal techniques to remove muscular artifacts, power line
273 noise, and other artifacts. Before analyzing the EEG data, it was subjected to preprocessing in which all the
274 possible artifacts (muscular, power line, head motion, and eye movement artifacts) that could contaminate the EEG
275 signal were removed as follows. Firstly, the MUSE EEG headband has an on-board noise cancellation mechanism
276 to filter out the noise based on the statistical properties of the data. The statistical properties used by the MUSE
277 headband include amplitude, variance, and kurtosis. An EEG signal is considered clean if its statistical properties
278 are below a predetermined threshold; otherwise, the signal is considered noisy and discarded. Furthermore, an SG
279 filter was used to smooth out the EEG signals that were recorded while keeping the strength of the signals. The
280 Savitzky-Golay (SG) filter is a good way to smooth out data because it is based on the least square polynomial
281 approximation principle (Savitzky and Golay, 1964). Different frequency (delta (0–4 Hz), theta (4–7 Hz), alpha
282 (8–12 Hz), beta (12–30 and beta-30) bands were used to translate the pre-processed EEG data into different

283 frequency bands using the MUSE on-board signal processing module. The mechanism used in this study for
284 the noise cancellation of the EEG signal has been found quite effective in several EEG studies in the
285 literature (Raheel et al., 2021, Raheel et al., 2020, Abd Rahman and Othman, 2016).

286 2.4 Data Analysis

287 The data was analyzed using SPSS version 22 (IBM Inc., Chicago, IL) and statistical analysis was performed based
288 on eight facial features for mental fatigue detection, including eye aspect ratio (EAR), eye distance (ED), eyebrow
289 distance (EBD), mouth aspect ratio (MAR), Nose to Jaw ratio (NJR), Nose to Chin ratio (NCR), Face Area (FA),
290 Head Motion (HM), NASA-TLX score, and EEG signals. Twenty-seven thousand frames were extracted from each
291 equipment operator's face during each experiment phase, and one value of each facial feature was calculated from
292 each frame, culminating in a dataset of twenty-seven thousand facial features for each equipment operator during
293 any experiment phase. After that, for descriptive representation, standard deviation (SD) and mean (M) values of
294 facial features for each phase of the experiment were computed. To analyze the variations in facial features due to
295 mental fatigue, we used general linear models for repeated measures. Four geometric measurements of each facial
296 feature were added as within-subjects factors: at baseline (T1), at 20 min (T2), at 40 min (T3), and at 60 min (T4).
297 Using partial eta-squared (η^2), we calculated the amount of the effect on the mean values of each characteristic and
298 the ground truth. Within-subject repeated measures analysis of variances (ANOVAs) was used for data analysis.
299 Consequently, the F distributions with degree of freedom was reported in the results. Furthermore, Benjamini-
300 Hochberg was also applied for multi-comparison corrections (Izmirlian, 2020) with a 5% false discovery rate (FDR)
301 or $q = 0.05$. Benjamini-Hochberg procedure is the most widely used statistical tool that increases the statistical

302 power and decreases the false discovery rate (Palejev and Savov, 2021). Pearson correlational coefficients were
303 used to assess the associations between the mean changes in geometric measurements of facial features throughout
304 the course of the experiment and the NASA-TLX scores to validate the proposed method. Furthermore, to develop
305 ecological validity for construction equipment operators, Pearson correlation coefficients were computed between
306 mean values of geometric measurements of facial features and EEG metric $[(\theta + \alpha) / (\alpha + \beta)]$. Because Tyas et al.
307 (2020) reported that such an EEG metric is the most used for computation of mental fatigue.

308 **3 Results**

309 In the study, all 16 construction equipment operators successfully completed the experiment. Therefore, data from
310 all operators was used for analysis.

311 *3.1 Analysis of ground truth data*

312 The NASA-TLX score was used as a ground truth for mental fatigue detection. Statistical analysis and descriptive
313 statistics of the ground truth assessment are shown in Table 3. The NASA-TLX demonstrated a substantial rise in
314 subjective mental fatigue, from 11.25 (SD = 2.77) at baseline (T-1) to 65.25 (SD = 4.85) at the end of the last
315 experiment phase (T-4). Table 3 shows that as the experiment progressed, operators reported increasing levels of
316 mental fatigue.

317 *3.2 Mental fatigue related facial metrics*

318 *3.2.1 Eye aspect ratio and eye distance:*

319 The descriptive statistics and statistical analysis of eye aspect ratio and eye distance-related facial features are
320 provided in Table 3 and Figure 4(a) and 4(b). The recorded results revealed a decrease in eye aspect ratio from

321 experiment phase T-1 (ratio = 0.517), T-2 (ratio = 0.465), T-3 (ratio = 0.380) to T4 (ratio = 0.306), whereas an
322 increase in eye distance feature was found from experiment phase T-1 (2.251 pixels), T-2 (2.317 pixels), T-3 (2.613
323 pixels) to T-4 (3.114 pixels). In general, the construction equipment operators showed a significantly decreasing
324 eye aspect ratio due to mental fatigue (GLM: $F(3, 45) = 25.597$, $p < 0.05$, partial $\eta_p^2 = 0.631$). Furthermore,
325 significant differences in pairwise comparisons was found for eye aspect ratio, between the experiment phases i.e.,
326 T1-T2 ($t_{Stat} = 4.040$, $p = 0.001$), T2-T3 ($t_{Stat} = 2.785$, $p = 0.014$), T3-T4 ($t_{Stat} = 2.917$, $p = 0.011$), T1-T3
327 ($t_{Stat} = 3.821$, $p = 0.002$), T1-T4 ($t_{Stat} = 8.007$, $p < 0.001$), and T2-T3 ($t_{Stat} = 8.611$, $p < 0.001$) using
328 Benjamini-Hochberg corrections, shown in Table 4. Nevertheless, the pattern was increasing ($F(3, 45) = 12.919$,
329 $p < 0.05$, partial $\eta_p^2 = 0.463$) for eye distance feature, Likewise, using Benjamini-Hochberg multi-comparison
330 corrections, significant differences for ED were also found in pairwise comparisons between the experiment phases,
331 i.e., T1-T4 ($t_{Stat} = -11.635$, $p < 0.001$), and T2-T4 ($t_{Stat} = -8.247$, $p < 0.001$), shown in Table 4. However,
332 through paired comparisons in the rest of the experiment phases for eye distance, it was discovered that the
333 differences were not significant. The boxplots of the data statistics for both eye aspect ratio and eye distance are
334 shown in Figures 5(a) and 5(b), respectively. Attributable to low R^2 values, the variations in these features are due
335 to the mental fatigue of operators, as reflected by the regression analysis displayed in Figure 6 of these two facial
336 traits with other features.

337 3.2.2 Eyebrows

338 Table 3 and Figure 4(c) provide the descriptive statistics and statistical analysis of eyebrow-related facial features.

339 This feature is a sum of the Euclidean distance between the anchor landmark on the nose and the corresponding

340 landmarks on the eyebrows. The results indicate that the average value of the eyebrow feature increased from
341 experiment phase T-1 (5.976 pixels), T-2 (6.071 pixels), T-3 (6.276 pixels) to T4 (6.448 pixels). There were also
342 significant main effects of time-on-task on eyebrow features (GLM: $F(3, 45) = 17.636, p < 0.05, \text{partial } \eta_p^2 =$
343 0.540). Besides, the pairwise comparisons of eyebrow features with Benjamini-Hochberg showed significant
344 differences for Eyebrow between the experiment phases, i.e., T1-T2 ($t_{Stat} = -4.268, p = 0.001$), T1-T3 ($t_{Stat} =$
345 $-4.463, p < 0.001$), T1-T4 ($t_{Stat} = -5.771, p < 0.001$), T2-T3 ($t_{Stat} = -3.105, p = 0.007$), and T2-T4 ($t_{Stat} =$
346 $-5.184, p < 0.001$), shown in Table 4. However, the corrections for the rest of the comparisons were not significant.
347 Besides, Figure 4(c) indicates that the average Euclidean distance for eyebrow characteristics rose from experiment
348 phase T-1 at baseline to experiment phase T-4. Figure 5(c) depicts the boxplots of the data statistics for the eyebrow
349 feature for all experiment phases.

350 3.2.3 Mouth Aspect Ratio

351 Table 3 and Figure 4(f) provide the descriptive statistics and statistical analysis of mouth aspect ratio related facial
352 features. The results indicate that there was an increase in mouth aspect ratio from experiment phase T-1 (ratio =
353 0.301), T-2 (ratio = 0.314), T-3 (ratio = 0.318) to T4 (ratio = 0.329). Considerable main effects of time on task
354 were also found on mouth aspect ratio (GLM: $F(3, 45) = 31.390, p < 0.05, \text{partial } \eta_p^2 = 0.677$). Subsequent pairwise
355 comparisons with Benjamini-Hochberg corrections showed notable differences in mouth aspect ratio for each of
356 the experiment phases i.e., T1-T2 ($t_{Stat} = -6.584, p < 0.001$), T1-T3 ($t_{Stat} = -9.511, p < 0.001$), T1-T4 (t_{Stat}
357 $= -7.026, p < 0.001$), T2-T3 ($t_{Stat} = -2.516, p = 0.024$), T2-T4 ($t_{Stat} = -4.524, p < 0.001$), and T3-T4 (t_{Stat}
358 $= -2.686, p = 0.017$), shown in Table 4. However, the rest of the pairwise comparisons were not statistically

359 significant. The pairwise comparison also indicated that the mean value of the mouth aspect ratio at baseline was
360 significantly shorter than at rest of the experiment phases. As shown in Figure 4(f), all other pairwise comparisons
361 were not statistically significant. Moreover, Figure 5(d) depicts boxplots of the mouth aspect ratio data statistics
362 for each experiment phase. Attributable to low R^2 values, it can be concluded that the variation in mouth aspect
363 ratio is due to the mental fatigue of operators, as depicted by the regression analysis displayed in Figure 6 of this
364 trait with other features.

365 *3.2.4 Nose to Jaw Ratio and Nose to Chin Ratio*

366 Table 3, Figures 4(d) and 4(e) provide the descriptive statistics and statistical analysis of nose-to-jaw ratio and
367 nose-to-chin ratio related facial features. The results indicate that the variation in nose-to-jaw ratio was not
368 monotonous during the experiment phases; T-1 (ratio = 3.272), T-2 (ratio = 3.235), T-3 (ratio = 3.249) to T4 (ratio
369 = 3.163), whereas a decrease pattern was found in the mean value of nose-to-chin ratio during the experiment
370 phases; T-1 (ratio = 2.119), T-2 (ratio = 2.058), T-3 (ratio = 1.897) to T-4 (ratio = 1.841). Considerable main effects
371 of time on task on the nose-to-jaw ratio (GLM: $F(3, 45) = 1.067, p > 0.05$, partial $\eta_p^2 = 0.066$) was not found.
372 Nevertheless, the construction equipment operators showed a significantly decreasing nose to chin ratio due to
373 mental fatigue (GLM: $F(3, 45) = 12.627, p < 0.05$, partial $\eta_p^2 = 0.457$) with significant differences in pairwise
374 comparisons was found using Benjamini-Hochberg corrections, between the experiment settings i.e., T1-T2 (t_{Stat}
375 = 3.037, $p = 0.008$), T1-T3 ($t_{Stat} = 4.836, p < 0.001$), T1-T4 ($t_{Stat} = 4.041, p = 0.001$), and T2-T3 ($t_{Stat} =$
376 3.949, $p = 0.001$), T2-T4 ($t_{Stat} = 3.431, p = 0.004$), shown in Table 4. However, the pairwise comparisons for
377 NTC were not statistically significant between the last two experiment phases, i.e., T3 and T4. Furthermore,

378 Figures 5(e) and 5(f) show boxplots of data statistics for nose to chin ratio and nose to jaw ratio across all
379 experiment phases.

380 3.2.5 Face Area and Head Motion

381 Table 3, Figures 4(g) and 4(h) provides the descriptive statistics and statistical analysis of face area and head
382 motion related facial features. The results indicate that there was an increase in the mean values of face area (FA)
383 feature from experiment phase T-1 (8.653 pixels²), T-2 (9.077 pixels²), T-3 (10.461 pixels²) to T4 (11.705 pixels²).
384 Besides, an increase in the mean value of head motion (HM) feature was also recorded from experiment phase T-
385 1 (5.659 pixels/frame), T-2 (5.807 pixels/frame), T-3 (6.006 pixels/frame) to T-4 (6.149 pixels/frame). During the
386 excavation operation, a significantly increasing pattern was found in the geometrical measurements of both the
387 facial features i.e., face area (GLM: $F(3, 45) = 24.444, p < 0.05$, partial $\eta_p^2 = 0.620$) and head motion (GLM: $F(3,$
388 $45) = 32.546, p < 0.05$, partial $\eta_p^2 = 0.685$). Subsequently, pairwise comparisons with Benjamini-Hochberg
389 corrections showed significant difference in the mean values of FA for all the experiment settings i.e., T1-T2 (t_{Stat}
390 $= -5.238, p < 0.001$), T1-T3 ($t_{Stat} = -5.192, p < 0.001$), T1-T4 ($t_{Stat} = -7.215, p < 0.001$), T2-T3 ($t_{Stat} = -$
391 $3.911, p = 0.001$), T2-T4 ($t_{Stat} = -5.924, p < 0.001$), and T3-T4 ($t_{Stat} = -2.208, p = 0.043$), shown in Table
392 4. Similarly, using Benjamini-Hochberg multi-comparison corrections, significant differences in pairwise
393 comparisons were found for head motions between the experiment phases, i.e., T1-T2 ($t_{Stat} = -6.657, p < 0.001$),
394 T1-T3 ($t_{Stat} = -6.635, p < 0.001$), T1-T4 ($t_{Stat} = -9.328, p < 0.001$), T2-T3 ($t_{Stat} = -4.423$, and $p < 0.001$),
395 and T2-T4 ($t_{Stat} = -5.684, p < 0.001$). However, the rest of pairwise comparisons for both the facial features
396 were not significant. The boxplots of the data statistics for face area and head motion during all phases of the

397 experiment are shown in Figures 5(g) and 5(h). Due to low R2 values, it can be concluded that the changes in these

398 traits are due to mental fatigue of operators, as demonstrated by the regression analysis showed in Figure 6.

399 Table 3: Means and standard deviations of mental fatigue metrics in different time phases

Metrics	Time			
	Baseline (T1)	20 mins (T2)	40 mins (T3)	60 mins (T4)
Subjective Assessment				
NASA-TLX Score (0-100)	11.25 (2.77)	30.81 (2.99)	45.00 (4.27)	65.25 (4.85)
Facial Features				
Eye Aspect Ratio	0.517 (0.116)	0.465 (0.086)	0.380 (0.103)	0.306 (0.024)
Eye Distance (pixels)	2.251 (0.523)	2.317 (0.532)	2.613 (0.783)	3.114 (0.681)
Eyebrow (pixels)	5.976 (0.582)	6.071 (0.595)	6.276 (0.778)	6.448 (0.777)
Mouth Aspect Ratio	0.301 (0.013)	0.314 (0.014)	0.318 (0.013)	0.329 (0.016)
Nose to Jaw Ratio	3.272 (0.166)	3.235 (0.153)	3.249 (0.255)	3.163 (0.277)
Nose to Chin Ratio	2.119 (0.604)	2.058 (0.576)	1.897 (0.569)	1.841 (0.478)
Face Area (pixels ²)	8.653 (0.809)	9.077 (0.857)	10.461 (1.606)	11.705 (2.128)
Head Motion (pixels per frame)	5.659 (0.166)	5.807 (0.161)	6.006 (0.295)	6.149 (0.322)

400

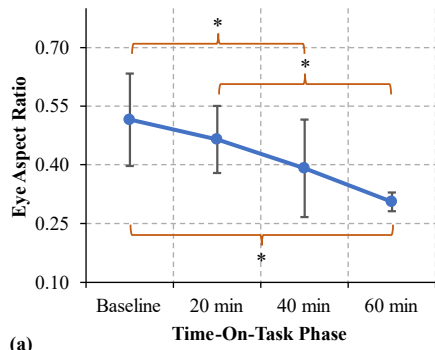
401 Table 4: Significance of facial feature with respect to various timepoints

Metrics	ANOVA		η^2	Multi-Comparison Corrections using Benjamini-Hochberg					
	F	P		T1 vs T2	T1 vs T3	T1 vs T4	T2 vs T3	T2 vs T4	T3 vs T4
EAR	25.597	≤ 0.05	0.631	4.040*	3.821*	8.007*	2.785*	8.611*	2.917*
ED	12.919	≤ 0.05	0.463	-0.841	-2.101	-11.635*	-1.359	-8.247*	-2.348
EB	17.636	≤ 0.05	0.540	-4.268*	-4.463*	-5.771*	-3.105*	-5.184*	-1.810
MAR	31.390	≤ 0.05	0.677	-6.584*	-9.511*	-7.026*	-2.516*	-4.524*	-2.686*
NJR	1.067	≥ 0.05	0.066	-	-	-	-	-	-
NCR	12.627	≤ 0.05	0.457	3.037*	4.836*	4.041*	3.949*	3.431*	0.957
FA	24.444	≤ 0.05	0.620	-5.238	-5.192*	-7.215	-3.911*	-5.924*	-2.208*
HM	32.546	≤ 0.05	0.685	-6.657*	-6.635*	-9.328*	-4.423*	-5.684*	-1.919

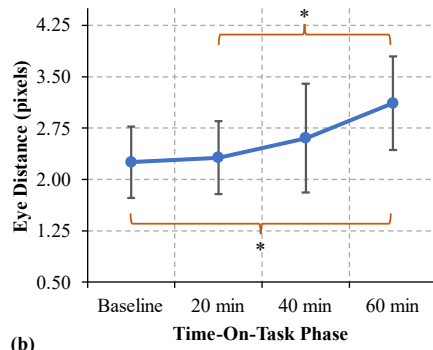
*EAR is Eye Aspect Ratio; ED is Eye Distance; EB is Eyebrow; MAR is Mouth Aspect Ratio; NJR is Nose to Jaw Ratio; NCR is Nose to Chin Ratio; FA is Face Area; HM is Head Motion; η^2 is effect size Partial eta-squared; *The t_{stat} is significant at the $p < 0.05$*

402

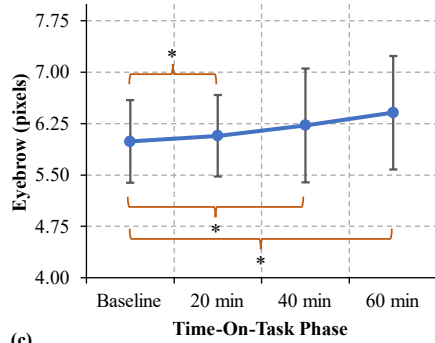
403



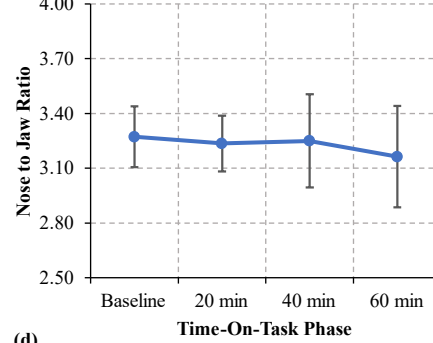
(a)



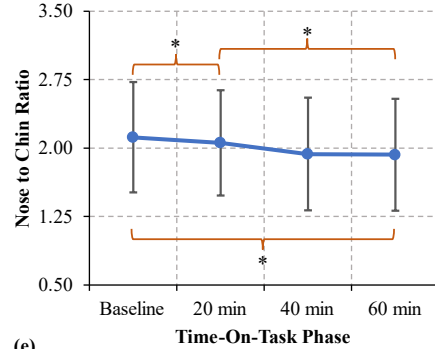
(b)



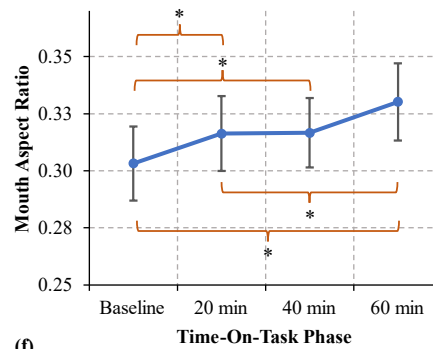
(c)



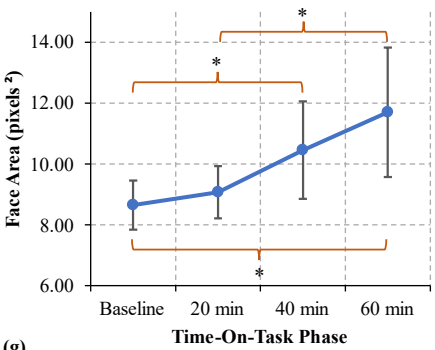
(d)



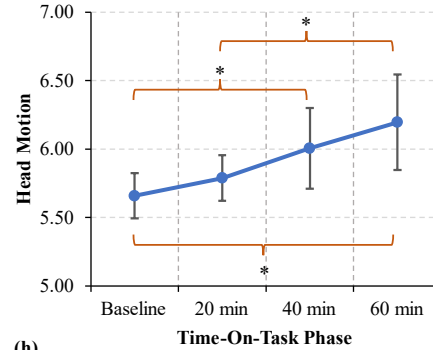
(e)



(f)



(g)



(h)

Figure 4: Variation in facial features due to mental fatigue with increasing Time-On-Task phases, (a) eye aspect ratio; (b) eye distance; (c) eyebrow; (d) nose to jaw ratio; (e) nose to chin ratio; (f) mouth aspect ratio; (g) face area; (h) head motion

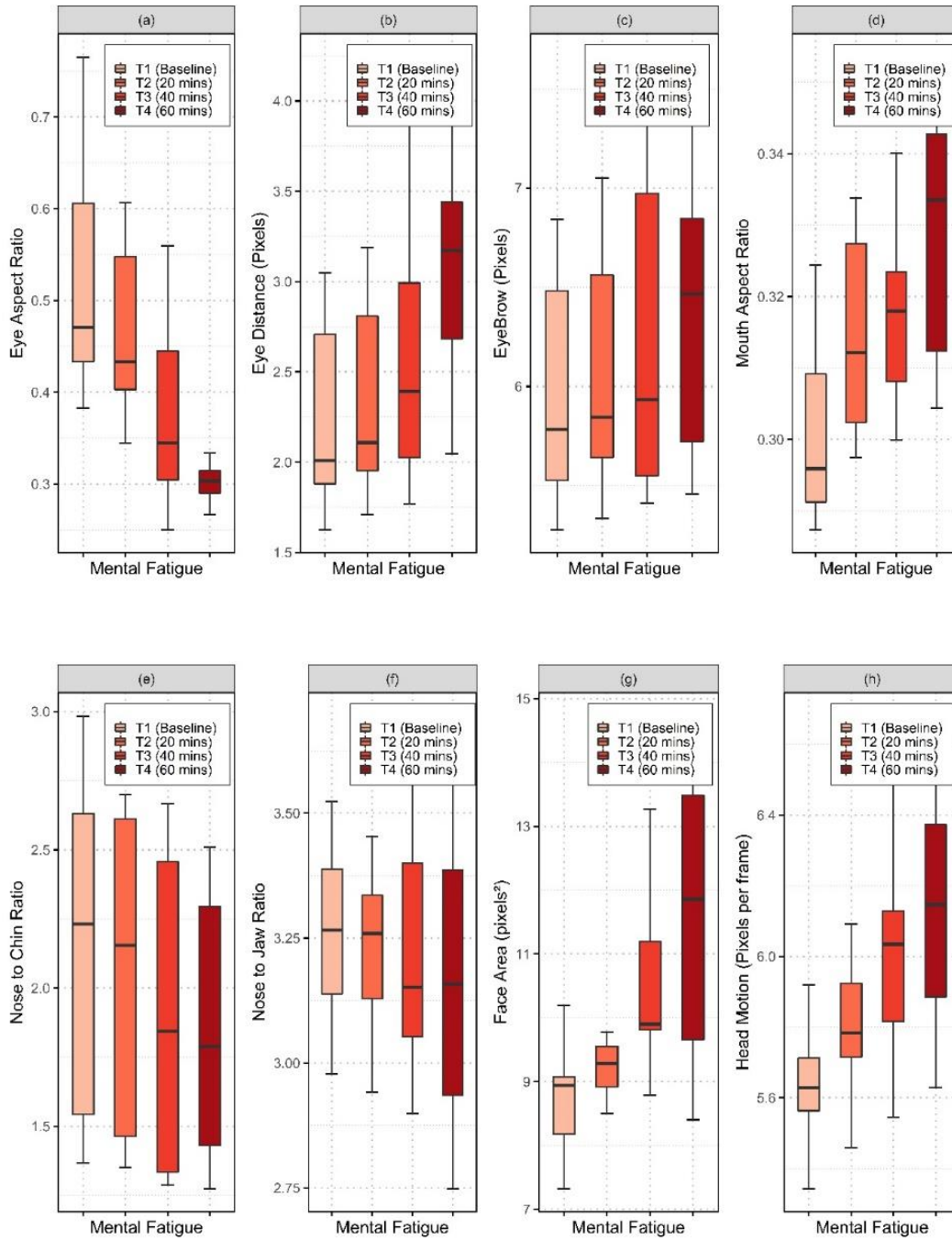


Figure 5: Boxplots for facial features (a) eye aspect ratio (b) eye distance (c) eyebrow (d) mouth aspect ratio (e) nose to chin ratio (f) nose to jaw ratio (g) face area and (h) head motion

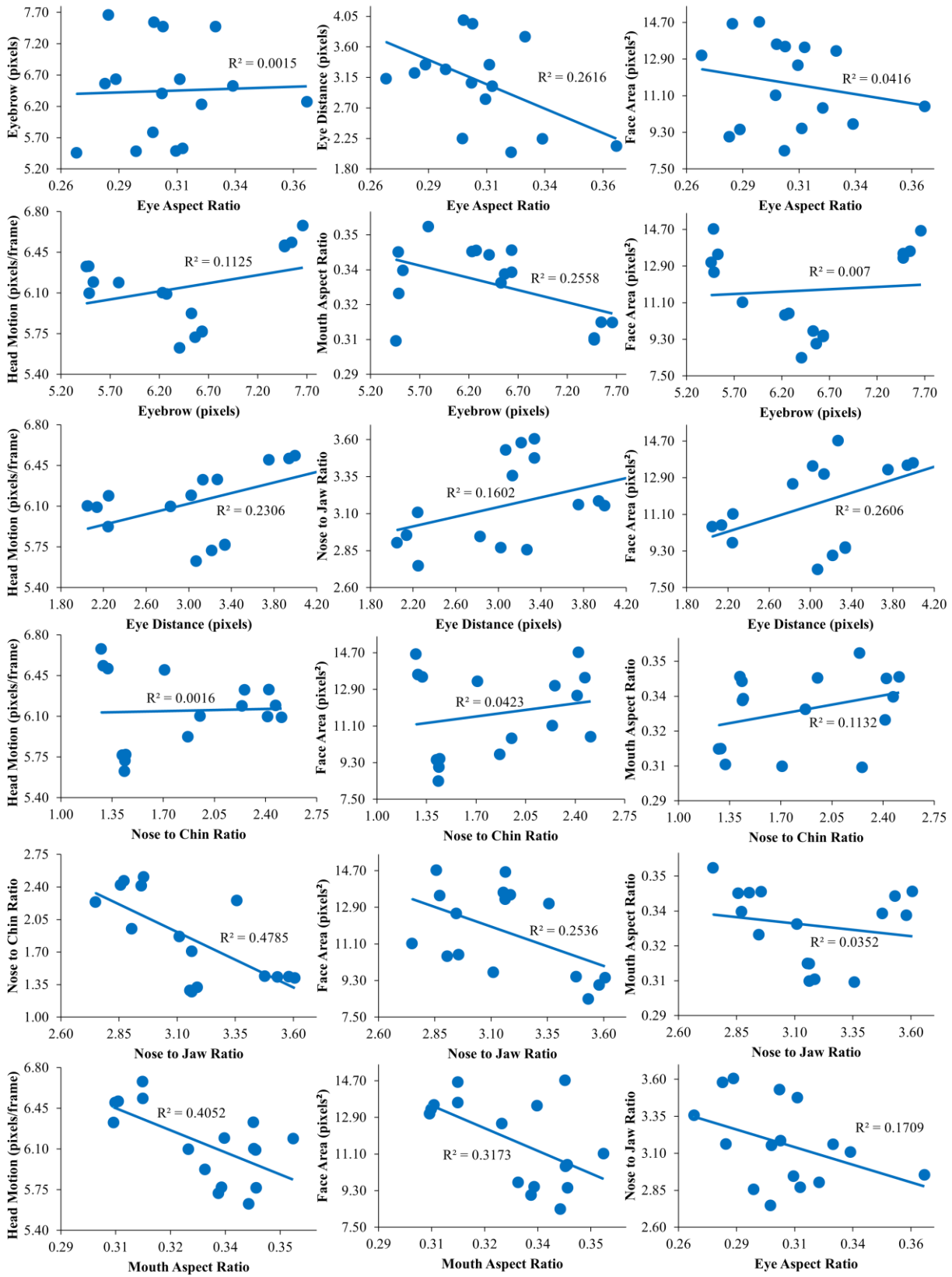


Figure 6: Regression statistics between individual facial features at the end of experiment

408 3.3 *Analysis of physiological data*

409 Analysis of the physiological signals EEG was performed by applying the paired t-test on the absolute power for
410 each frequency band of the EEG signal obtained from all the channels of the MUSE headband during the four
411 experimental phases: baseline, at 20 min, 40 min, and 60 min. A null hypothesis and p-value were used to determine
412 the t-test decision. The difference between the groups was considered significantly different if the p-value was less
413 than 0.05 and the null hypothesis was 1. Table 5 shows a statistically significant difference according to the results
414 of *p*-value for EEG power spectral density in different brain regions. For example, the *t*-test applied to EEG signals
415 revealed that the alpha band was found to be statistically significant at right frontal channel AF8 (between all
416 experiment phases at baseline and 20 mins; 20 mins and 40 mins) and at left frontal channel AF7, it was statistically
417 significant between experiment phases 20 mins and 40 mins only. Likewise, the beta band was found to be
418 statistically significant at left frontal channel AF7 (between experiment phases at 40 mins and 60 mins only) and
419 frontal channel AF8 between all experiment phases. The Delta and gamma bands were found to be statistically
420 significant in the left and right temporal regions. The beta band, on the other hand, showed differences that were
421 statistically significant in both the frontal and temporal parts of the brain. The statistical analysis for all the bands
422 in the respective channels is demonstrated in Table 5. Figure 7 shows the brain activity visualization obtained
423 using the power spectral density of the EEG data of the construction equipment operators during the four phases
424 of the experiment. On the brain maps, the red color shows strong cortical activity, while the orange color shows
425 little brain activity. It can be observed from the brain maps that the alpha and beta bands of AF7 and AF8 frontal
426 channels have visually distinct brain activity at baseline, 20 min, 40 min, and 60 min of the experiment.

Table 5: p -value for EEG power spectral densities in different brain regions

Time	Channels	EEG Frequency Bands (p values by t -test)				
		Delta	Theta	Alpha	Beta	Gamma
T1 – T2 (0 & 20 min)	AF7	7.011E-09*	0.00071*	0.06148	0.62845	0.09649
	AF8	2.924E-09*	1.438E-09*	0.04877*	1.345E-05*	2.519E-05*
	TP9	3.425E-05*	0.45987	0.56974	0.00568*	1.671E-17*
	TP10	0.00167*	2.883E-07*	1.446E-10*	1.959E-12*	7.304E-13*
T2 – T3 (20 & 40 min)	AF7	4.214E-05*	0.55471	0.00023*	0.76902	0.08094
	AF8	0.60858	0.00053*	0.00016*	3.219E-06*	0.13631
	TP9	0.02326*	0.52230	0.20485	1.716E-06*	0.18105
	TP10	0.01776*	0.98454	0.19671	0.12579	1.678E-11*
T3 – T4 (40 & 60 min)	AF7	0.13977	0.71663	0.97207	0.00155*	0.00023*
	AF8	0.00480*	0.00295*	0.00241*	0.00026*	0.00024*
	TP9	0.00882*	0.00046*	0.01284*	0.00357*	0.00627*
	TP10	0.01746*	5.106E-05*	0.17877	0.00441*	0.00289*

*The mean difference is significant at the 0.05 level

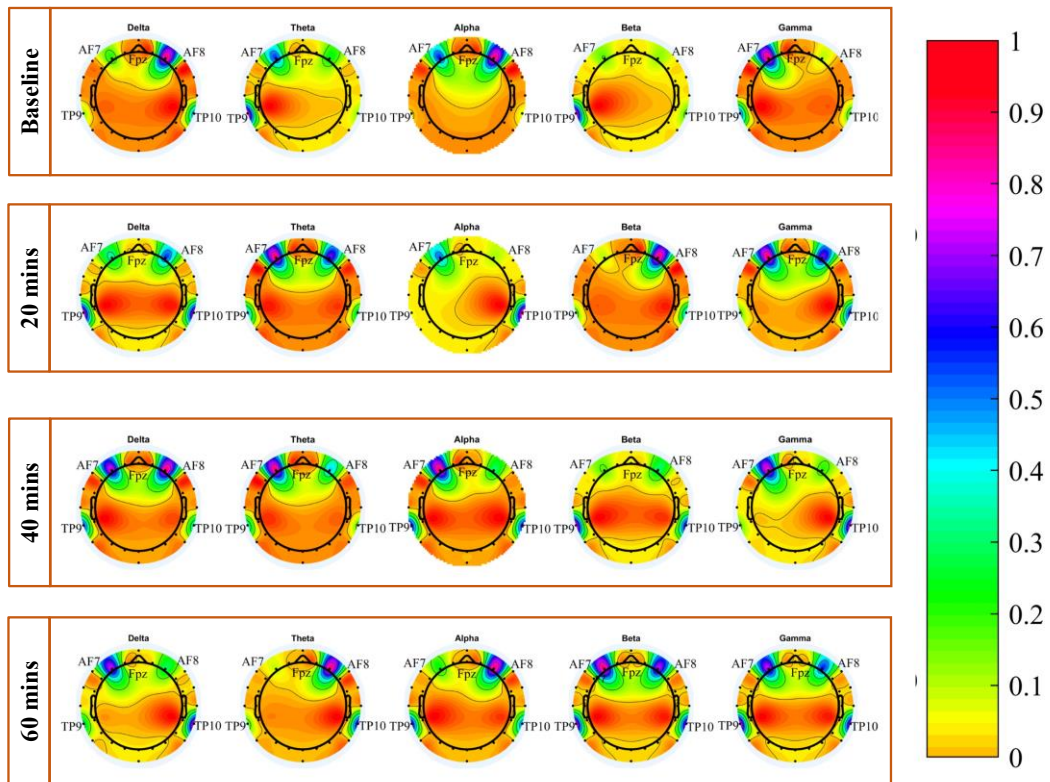


Figure 7: Brain activity visualization in terms of power spectral density of different EEG bands for the four experiment phases

429 3.4 *Validity of the facial features' geometric measurements*

430 3.4.1 *Correlations between facial features' geometric measurements and subjective mental fatigue scores*

431 In Table 6, correlations between geometric measurements of facial features and subjective mental fatigue scores
 432 are shown. The eye aspect ratio at T-1 ($r = -0.5202$), T-3 ($r = -0.6730$), and T-4 ($r = -0.5760$) minutes of the
 433 experiment was significantly correlated with the corresponding subjective mental fatigue scores. Similarly,
 434 geometric measurements of eye distance facial features were significantly associated with subjective mental
 435 fatigue scores during all the experiment phases; T-1 ($r = 0.7164$), T-2 ($r = 0.5029$), T-3 ($r = 0.6866$) and T-4 ($r =$
 436 0.9264). Furthermore, across all experiment phases, the head motion face feature was substantially linked with the
 437 corresponding subjective scores. However, mouth aspect ratio was only correlated at T-4 ($r = -0.5872$). Also, at
 438 experiment phases T3 ($r = 0.5884$) and T-4 ($r = 0.5078$), face area feature was related. However, there was no
 439 association between the remaining facial features (e.g., eyebrows, nose to chin ratio, and nose to jaw ratio) and
 440 subjective mental fatigue.

441 **Table 6: Correlations between facial features and subjective scores of mental fatigues**

Parameters	NASA-TLX Score				
	Time	Baseline	20 min	40 min	60 min
Eye Aspect Ratio	Baseline	-0.5202*			
	20 min		-0.4635		
	40 min			-0.6730**	
	60 min				-0.5760*
Eye Distance (Pixels)	Baseline	0.7164**			
	20 min		0.5029*		
	40 min			0.6866**	
	60 min				0.9264**
Eyebrow (Pixels)	Baseline	0.6318**			
	20 min		0.7327**		

	40 min		0.5695*	
	60 min			0.5967*
Mouth Aspect Ratio	Baseline	0.0075		
	20 min		0.0762	
	40 min		0.2226	
	60 min			-0.5872*
Nose to Jaw Ratio	Baseline	0.1448		
	20 min		0.0241	
	40 min		0.4504	
	60 min			0.2912
Nose to Chin Ratio	Baseline	-0.6134*		
	20 min		-0.5954*	
	40 min		-0.5288*	
	60 min			-0.6011*
Face Area (Pixels ²)	Baseline	0.1313		
	20 min		0.1382	
	40 min		0.5884*	
	60 min			0.5078*
Head Motion (Pixels per frame)	Baseline	0.5209*		
	20 min		0.6910**	
	40 min		0.5003*	
	60 min			0.5413*

**Correlation is significant at 0.05; **Correlation is significant at 0.01*

442 *3.4.2 Correlations between facial features' geometric measurements and EEG metric*

443 The correlations between facial features and electroencephalography metric $[(\theta + \alpha) / (\alpha + \beta)]$ for mental fatigue
444 are shown in Table 7. The eye aspect ratio was significantly correlated with EEG during all the experiment phases,
445 i.e., at baseline ($r = 0.6849$), 20 min ($r = 0.5008$), 40 min ($r = 0.5510$), and 60 min ($r = -0.5760$) of the experiment.
446 Similarly, geometric measurements of head motion facial features during experiment phases; at baseline ($r = -$
447 0.5042), 20 min ($r = -0.6234$), 40 min ($r = -0.5374$), and 60 min ($r = -0.4985$) were significantly associated with
448 the EEG metric. Furthermore, at baseline, 20 minutes, and 60 minutes of the experiment, the eye distance facial

449 feature was found to be significantly linked with the EEG metric. The findings also revealed that eye aspect ratio
 450 was positively associated, whereas the eye distance and head motion facial features were negatively correlated with
 451 the EEG metric. However, the correlation of rest of the facial features with EEG metric was not monotonous during
 452 all the experiment phases as shown in Table 7.

453 **Table 7: Correlation between EEG metric and facial features**

Facial Features	EEG Metric $[(\theta + \alpha) / (\alpha + \beta)]$			
	Baseline	20 mins	40 mins	60 mins
Eye Aspect Ratio	0.6849*	0.5008*	0.5510*	0.6505*
Eye Distance	-0.6701*	-0.3608	-0.5497*	-0.7155*
Eyebrow	-0.5698*	-0.6034*	-0.4507	-0.2246
Nose to Jaw Ratio	-0.4007	-0.3472	-0.3618	-0.1323
Nose to Chin Ratio	0.5861*	0.4915	0.4717	0.2269
Mouth Aspect Ratio	0.1600	0.4466	0.1282	0.3830
Face Area	-0.1311	-0.3872	-0.5566*	-0.5881*
Head Motion	-0.5042*	-0.6234*	-0.5374*	-0.4985*

**Correlation is significant at the 0.05 level*

454 **4 Discussion**

455 The current study is the first of its kind in the construction industry because of its non-invasive methodology.
 456 According to the results of the subjective assessment and variations in geometric measurements of facial features,
 457 individuals experienced increasing mental fatigue after participating in the experiment phases. The findings are
 458 statistically significant and support the idea of monitoring mental fatigue using geometric measurements of facial
 459 features. As far as the authors know, no study has compared the proposed method to invasive methods like
 460 electroencephalography that are used to monitor mental fatigue in construction equipment operators.

461 *4.1 Variations in the facial features' geometric measurements*

462 The findings of this research are in line with those conducted in non-construction domains that have utilized facial

463 features for mental fatigue detection. The current study used geometric measurements of eight facial features: eye
464 aspect ratio, eye distance, eyebrow, nose to chin ratio, nose to jaw ratio, mouth aspect ratio, and head motion.
465 Comparable studies in non-construction domains have used eye-related variables for mental fatigue detection with
466 similar findings. There was a statistically significant difference in eye aspect ratio and eye distance. From baseline
467 until the end of the experiment, they demonstrated a rise in the mean values of eye distance and a decrease in the
468 mean values of eye aspect ratio. The variation in mean values reveals that landmarks were moved closer together
469 as mental fatigue increased among equipment operators. Therefore, such a variation pattern is suggestive of
470 increased blinking and eye closure due to increased mental fatigue. Hence, the construction equipment operators'
471 cognitive effort increased. Likewise, the study found an increase in the eyebrow. However, the increase was not
472 statistically significant. The results are aligned with the previous studies that showed an increase in the blinking
473 of eyes during fatigue states. For example, Giannakakis et al. (2017) and Norzali et al. (2014) reported an increase
474 in the blink rate under stressful situations and concluded that blink rate and mental stress are highly correlated
475 with each other. Nevertheless, Wenhui et al. (2005) reported that the eye blinks decreased with an increase in
476 cognitive effort. A change in eye metrics was also found by Bevilacqua et al. (2018) in a study where subjects were
477 subjected to stressful scenarios of a game. Likewise, Ravaja et al. (2006) also stated an increase in orbicularis oculi
478 (a muscle associated with eyelid movement) electromyography activity in non-neutral emotional states. Our study
479 found no statistically significant differences in eyebrow activity among operators, although the variation is
480 consistent with earlier research. For example, a study by Kimmelman et al. (2020) stated that eyebrow positions
481 are affected by emotional states.

482 Mouth-related features of construction equipment operators appear to be indicators of mental fatigue. This study
483 demonstrated an increase in the mean mouth aspect ratio from baseline to the last experiment phase. The increase
484 was statistically significant. The increase in mean values indicates that the position of mouth landmarks strayed
485 away from each other due to increased mental fatigue. Similarly, such a change may be indicative of frequent
486 mouth movements with an increase in mental fatigue. For example, a study by Giannakakis et al. (2017) reported
487 that an increased variation and median of the highest magnitude of mouth activity imply faster mouth movements
488 during stressful conditions. Similarly, as studied by Tang et al. (2016), the mouth remains closed in a normal state
489 while it opens when a subject is in fatigued state. Likewise, Tijs et al. (2008) reported that in emotional states, the
490 zygomatic (a face muscle that is linked to the mouth) is more active.

491 Mental fatigue also affects facial traits linked to construction equipment operators' dynamic body motions, such
492 as head motion, face area, nose to chin ratio, and nose to jaw ratio. Bevilacqua et al. (2018) stated these dynamic
493 body movements as head movement and physical posture. The operator's head moves vertically, horizontally, and
494 rotationally while operating. Thus, the increase in the mean value of this feature demonstrates that as the
495 experiment progressed, the operators' head motion increased due to mental fatigue. Table 3 shows the change,
496 which is statistically significant throughout all experiment stages, indicating greater mental fatigue. Similarly, the
497 current study analyzed nose to jaw and nose to chin ratios. The preceding was to represent the face's shift to the
498 right or left. The latter feature reflected the operator's face tilting upward or downward. The mean nose to chin
499 ratio decreased from the baseline to the completion of the excavation experiment. It is because the operators were
500 advancing towards the camera, but their faces were tilted upwards, indicating they were attempting to keep their

501 focus on the task despite fatigue. However, the differences between the phases were not statistically significant.
502 The present study's findings accord with past research in other sectors. For example, Liao et al. (2005) and Dinges
503 et al. (2005) found an increase in head movements during non-neutral states. Furthermore, studies by Kusano et
504 al. (2020), Giannakakis et al. (2018), and Giannakakis et al. (2017) also reported an increased head motion under
505 stressful situations such as watching videos. Nevertheless, results from the current study are contrary to the
506 findings by Bevilacqua et al. (2018), where no statistical significance was reported between boring and stressful
507 states.

508 Additionally, the current study also studied the face area feature which was associated with the movement of
509 equipment operators towards and away from the camera. The current study demonstrated an increase in face area,
510 indicating the movement of operators towards the camera. The increase between the subsequent experiment phases
511 from baseline was 4.90%, 15.24%, and 11.89%, respectively. The findings are consistent with the previous study
512 by Bevilacqua et al. (2018) where there was an increase in the face area of subjects during a stressful state.

513 *4.2 Relationship of facial features' geometric measurements with subjective and objective assessment*

514 During the excavation operation experiment, there were strong relationships between geometric measurements of
515 facial features and subjective mental fatigue scores. Some variables correlated with subjective scores throughout
516 the entire experiment, while others only correlated at one or two stages. For example, face area features were
517 substantially linked with subjective scores during the final two experiment phases, i.e., at 40 and 60 minutes,
518 shown in Table 6. Previous studies have found that fatigue assessments are substantially connected to eye-related
519 cues (Sundelin et al., 2013). Likewise, a study by Hopstaken et al. (2015) also reported an increase in subjective

520 mental fatigue and a decrease in baseline pupil diameter as a result of increasing time spent on the activity, with a
521 corresponding decrease in cognitive performance. Similarly, a study by Dziuda et al. (2021) also found that the
522 drivers' responses to the fatigue symptoms scale questionnaire before and after the simulator task were found to
523 be correlated with changes in their percentage closure of eye time levels.

524 This study found a difference between EEG bands (baseline, 20 min, 40 min, and 60 min) in the evolution of
525 mental fatigue. After an hour of continuous operation of construction equipment, we found alterations in
526 spontaneous brain activity. Five EEG patterns were evaluated in four brain areas: AF7, AF8, TP9, and TP10. Figure
527 4 shows the brain maps using the power spectral density of EEG data from construction equipment operators at
528 the outset, 20 minutes, 40 minutes, and 60 minutes of the experiment. The beta band's power covers the entire
529 brain. The temporal delta and gamma bands revealed a consistent trend. The frontal alpha band rhythm was not
530 monotonous. Figure 4 depicts the frontal and temporal lobes of the brain becoming fatigued as the experiment
531 progressed. In some areas, the theta band colors are redder and bluer. The p-values for statistical significance are
532 also monotonous. The findings are consistent with previous research on fatigue (Li et al., 2020a, Eoh et al., 2005).
533 Theta waves, which are linked to brain fatigue, appear early in the sleep cycle, making them sensitive to mental
534 fatigue (Lal and Craig, 2005, Åkerstedt and Gillberg, 1990). Alpha rhythm indicates the condition of relaxation
535 and wakefulness (Li et al., 2020a). In the third and fourth experiment phases of the study, alpha activity was
536 observed in the frontal channels shown, in Figure 4, which is in line with previous research. For example, studies
537 by Eoh et al. (2005) and Lal and Craig (2002) reported that the potency of the alpha pattern increases with an
538 increase in mental fatigue. Similarly, another study by Sun et al. (2014) and Craig et al. (2012) also reported that

539 with an increase in mental fatigue, the power of the alpha band increases. This is why it is considered the most
540 reliable indication of mental fatigue (Lal and Craig, 2005). During the excavation operation experiment, there
541 were strong relationships between geometric measurements of facial features and EEG metric. Some variables
542 corresponded with subjective scores throughout all experiment phases, while others correlated at one or two stages
543 only. For example, eye aspect ratio, eye distance, and head motion were substantially linked to the EEG metric
544 during all the experiment phases. As the construction equipment operators were subjected to mental fatigue, their
545 eye aspect ratio decreased, and their eye distance increased from the baseline. The decrease in eye aspect ratio
546 indicates the closing of eyes, thus indicating theta band activity in the brain topography. Likewise, the increase in
547 face area and head motion indicates that the equipment operators were trying to increase their concentration by
548 moving close to the windscreen of the equipment and camera. However, the association of the rest of the facial
549 features with the EEG metric was not found to be monotonous during each of the experiment phases. Overall,
550 geometric measures of facial features produce statistical conclusions that agree with the visual representations of
551 the brain as a result.

552 *4.3 Implications*

553 The proposed research study is expected to inspire changes in safety management practices on construction sites.
554 Using geometric measurements of the construction equipment operators' facial features, this study proposed a non-
555 invasive mental fatigue monitoring method that did not require the operators to wear sensors on their body. Apart
556 from determining the effectiveness of the proposed method, the study also compared the results with
557 electroencephalography (EEG), which is an invasive mental fatigue monitoring method. The findings of this

558 research have both practical and theoretical repercussions for alleviating the mental fatigue of construction
559 equipment operators. Firstly, the method being proposed herein, apart from detecting construction equipment
560 operators' mental fatigue, can also be useful for real-time facial features-based monitoring of mental fatigue on
561 construction sites. Thus, the findings of this study reveal that it is feasible to use geometric measurements of facial
562 features for mental fatigue detection during construction operations. Secondly, for construction managers, the
563 findings can help them develop a framework for managing shifts among workers. For one hour, the researchers in
564 the current study monitored changes in construction equipment operators' facial features and brain activity.
565 Equipment operators can be observed by managers every 30 or 45 minutes of construction work. Breaks between
566 shifts can be implemented to provide equipment operators a chance to rest and recuperate from the mental fatigue
567 they've triggered. Thirdly, the current method is non-invasive. It involves the use of a remote camera as a sensor
568 to take measurements of facial features without making physical contact. As a result, this method represents a
569 significant shift from earlier construction worker wearable sensor techniques such as those studied by Ke et al.
570 (2021b), Li et al. (2020b), Choi et al. (2019) and Hwang et al. (2018). Fourthly, as stated by Li et al. (2019b), the
571 rate of accretion of mental fatigue among equipment operators may be higher than the laboratory setting.
572 Consequently, the data collected for the study was from real construction sites. Therefore, the results advocate the
573 ecological validity of this method for construction equipment operators. As a result, geometric measures of facial
574 features open up new possibilities for contactless mental fatigue management among construction equipment
575 operators.

576 4.4 *Limitations and future research*

577 This study is the first of its kind to use geometric measurements of facial and EEG to monitor mental fatigue
578 among construction equipment operators, yet this study was subject to limitations that need to be addressed in
579 future research work. Firstly, this study studied temporal changes in the geometric measurements of facial features
580 at baseline, 20, 40, and 60 mins to monitor mental fatigue. The results were further validated by comparing them
581 with statistical analysis of the power spectral density of electroencephalography of construction equipment
582 operators. However, for future studies, a machine learning approach is advised to automatically identify the
583 geometric measurements of facial features. Furthermore, future studies are also recommended to calculate the
584 degree of mental fatigue by addressing its identification as a regression problem. Secondly, lighting fluctuations
585 are believed to have an impact on the geometric measurements of face feature detection (Tran et al., 2019, Lee et
586 al., 2018). To avoid this, we ran the experiments on the construction site at the same time each day for the
587 subsequent days under similar weather conditions. However, in future we intend to acquire to data at various times
588 throughout the day such as morning and evening, under varying weather conditions, to see how fluctuations in
589 lighting on construction sites affect the results connected to facial feature geometric measures and mental fatigue
590 monitoring. Thirdly, there may be a wide range of circumstances that can influence the appearance of a
591 construction equipment operator's facial features. It is imperative that future research explore the effects of age
592 (Boutet et al., 2015), experience, and other factors on the ability to discern mental fatigue based on facial features
593 during equipment operations. Lastly, this research only investigated geometric measurements of facial features
594 and EEG in equipment operators. Since there is no publicly available dataset for construction equipment operators
595 and because deep learning requires a lot of data, the current study does not apply deep learning techniques to

596 automatically identify mental fatigue. So, in the future, researchers might use recurrent neural networks (RNNs)
597 to track the mental fatigue of people who operate construction equipment by gathering a lot of data from real
598 construction sites.

599 **5 Conclusions**

600 Mental fatigue led attention failure of equipment operators is associated with the collisions between construction
601 equipment and surrounding site objects that lead to accidents causing injuries and fatalities. Therefore, the current
602 study developed a construction site procedure to detect construction equipment operators' mental fatigue, which
603 is a promising approach to mitigate the risk of equipment-related accidents. As a result, we performed an automated
604 analysis of geometric measures of facial features from video clips in conjunction with an empirical evaluation of
605 its applicability for construction equipment operators. To achieve this objective, 16 excavator operators were
606 engaged to record facial videos and EEG sensor data while working on an excavation activity. Eight distinct facial
607 features (eye aspect ratio, eye distance, eyebrows, mouth aspect ratio, nose to jaw ratio, nose to chin ratio, face
608 area, and head motion) comprised of Euclidean distance and areas were calculated from sixty-eight facial
609 landmarks. These facial features do not rely on 6 universal predefined facial expressions. Temporal values of these
610 facial features' geometric measurements and EEG sensor data were compared at baseline, 20 min, 40 min, and 60
611 min. The results indicate that there was a statistically significant difference in the mean values for all the facial
612 features (i.e., eye aspect ratio, eye distance, eye distance mouth aspect ratio, face area and head motion) between
613 various experiment phases at baseline, 20, 40, and 60 min. However, the results were not statistically significant
614 for the rest of the facial features. Consequently, the brain maps obtained using the power spectral density of the

615 EEG data recorded from construction equipment operators at the same time frames also advocate the fact that the
616 operators' brains were experiencing mental fatigue. The study's key contribution is to demonstrate the ecological
617 validity of contactless measures for detecting and evaluating mental fatigue for construction equipment operators
618 by studying their association with wearable EEG sensor data. The study found a strong association between the
619 proposed method and the electroencephalography metric. The proposed method's deployment is non-invasive and
620 based on video records. Furthermore, it does not require wearable sensing technology for mental fatigue
621 monitoring. Given the dynamic and complicated nature of construction site operations, it is believed that the
622 proposed methodology is more user-friendly, practical, and more appropriate to the construction domain for mental
623 fatigue monitoring. It will help to reduce equipment-related accidents, injuries, and errors on construction sites
624 through proactive monitoring of the operator's mental fatigue.

625 **Acknowledgement**

626 The authors acknowledged the following two funding grants: 1. General Research Fund (GRF) Grant (15201621)
627 titled "Monitoring and managing fatigue of construction plant and equipment operators exposed to prolonged
628 sitting"; and 2. General Research Fund (GRF) Grant (15210720) titled "The development and validation of a
629 noninvasive tool to monitor mental and physical stress in construction workers".

630 **References**

- 631 ABD RAHMAN, F. & OTHMAN, M. F. Real Time Eye Blink Artifacts Removal in Electroencephalogram Using
632 Savitzky-Golay Referenced Adaptive Filtering. *In: IBRAHIM, F., USMAN, J., MOHKOTAR, M. S. &*
633 *AHMAD, M. Y., eds. International Conference for Innovation in Biomedical Engineering and Life*
634 *Sciences, 2016// 2016 Singapore. Springer Singapore, 68-71.*
- 635 AHN, S., NGUYEN, T., JANG, H., KIM, J. G. & JUN, S. C. 2016. Exploring Neuro-Physiological Correlates of
636 Drivers' Mental Fatigue Caused by Sleep Deprivation Using Simultaneous EEG, ECG, and fNIRS Data.

637 *Frontiers in Human Neuroscience*, 10.

638 ÅKERSTEDT, T. & GILLBERG, M. 1990. Subjective and objective sleepiness in the active individual.

639 *International journal of neuroscience*, 52, 29-37.

640 ANSARI, S., NAGHDY, F., DU, H. & PAHNWAR, Y. N. 2022. Driver Mental Fatigue Detection Based on Head

641 Posture Using New Modified reLU-BiLSTM Deep Neural Network. *IEEE Transactions on Intelligent*

642 *Transportation Systems*, 23, 10957-10969.

643 ARAVIND, A., AGARWAL, A., JAISWAL, A., PANJIYARA, A. & SHASTRY, M. 2019. Fatigue detection system

644 based on eye blinks of drivers. *Int. J. Eng. Adv. Technol*, 8, 72-75.

645 ARSALAN, A., MAJID, M., BUTT, A. R. & ANWAR, S. M. 2019. Classification of Perceived Mental Stress

646 Using A Commercially Available EEG Headband. *IEEE Journal of Biomedical and Health Informatics*,

647 23, 2257-2264.

648 BACHURINA, V. & ARSALIDOU, M. 2022. Multiple levels of mental attentional demand modulate peak saccade

649 velocity and blink rate. *Heliyon*, 8, e08826.

650 BALTRUŠAITIS, T., ROBINSON, P. & MORENCY, L. OpenFace: An open source facial behavior analysis

651 toolkit. 2016 IEEE Winter Conference on Applications of Computer Vision (WACV), 7-10 March 2016

652 2016. 1-10.

653 BEVILACQUA, F., ENGSTRÖM, H. & BACKLUND, P. 2018. Automated Analysis of Facial Cues from Videos

654 as a Potential Method for Differentiating Stress and Boredom of Players in Games. *International Journal*

655 *of Computer Games Technology*, 2018, 8734540.

656 BOUTET, I., TALER, V. & COLLIN, C. A. 2015. On the particular vulnerability of face recognition to aging: a

657 review of three hypotheses. *Frontiers in Psychology*, 6.

658 CECH, J. & SOUKUPOVA, T. 2016. Real-time eye blink detection using facial landmarks. *Cent. Mach.*

659 *Perception, Dep. Cybern. Fac. Electr. Eng. Czech Tech. Univ. Prague*, 1-8.

660 CHEN, Y., LU, B., CHEN, Y. & FENG, X. 2015. Breathable and Stretchable Temperature Sensors Inspired by

661 Skin. *Scientific Reports*, 5, 11505.

662 CHENG, Q., WANG, W., JIANG, X., HOU, S. & QIN, Y. 2019. Assessment of Driver Mental Fatigue Using Facial

663 Landmarks. *IEEE Access*, 7, 150423-150434.

664 CHEW, J. Y., KAWAMOTO, M., OKUMA, T., YOSHIDA, E. & KATO, N. 2021. Multi-modal approach to

665 evaluate adaptive visual stimuli of remote operation system using gaze behavior. *International Journal of*

666 *Industrial Ergonomics*, 86, 103223.

667 CHOI, B., JEBELLI, H. & LEE, S. 2019. Feasibility analysis of electrodermal activity (EDA) acquired from

668 wearable sensors to assess construction workers' perceived risk. *Safety Science*, 115, 110-120.

669 CLB. 2020. "China Labour Bulletin - Worker Safety" available at: <https://clb.org.hk/content/work-safety> (accessed

670 on 14 August 2022).

671 CRAIG, A., TRAN, Y., WIJESURIYA, N. & NGUYEN, H. 2012. Regional brain wave activity changes associated

672 with fatigue. *Psychophysiology*, 49, 574-582.

673 DAS, S., MAITI, J. & KRISHNA, O. B. 2020. Assessing mental workload in virtual reality based EOT crane

674 operations: A multi-measure approach. *International Journal of Industrial Ergonomics*, 80, 103017.

675 DAZA, I. G., BERGASA, L. M., BRONTE, S., YEBES, J. J., ALMAZÁN, J. & ARROYO, R. 2014. Fusion of
676 optimized indicators from Advanced Driver Assistance Systems (ADAS) for driver drowsiness detection.
677 *Sensors*, 14, 1106-1131.

678 DINGES, D. F., RIDER, R. L., DORRIAN, J., MCGLINCHEY, E. L., ROGERS, N. L., CIZMAN, Z.,
679 GOLDENSTEIN, S. K., VOGLER, C., VENKATARAMAN, S. & METAXAS, D. N. 2005. Optical
680 computer recognition of facial expressions associated with stress induced by performance demands.
681 *Aviation, space, and environmental medicine*, 76, B172-B182.

682 DZIUDA, Ł., BARAN, P., ZIELIŃSKI, P., MURAWSKI, K., DZIWOSZ, M., KREJ, M., PIOTROWSKI, M.,
683 STABLEWSKI, R., WOJDAS, A., STRUS, W., GASIUL, H., KOSOBUDZKI, M. & BORTKIEWICZ,
684 A. 2021. Evaluation of a Fatigue Detector Using Eye Closure-Associated Indicators Acquired from Truck
685 Drivers in a Simulator Study. *Sensors*, 21, 6449.

686 EL KERDAWY, M., EL HALABY, M., HASSAN, A., MAHER, M., FAYED, H., SHAWKY, D. & BADAWI, A.
687 2020. The Automatic Detection of Cognition Using EEG and Facial Expressions. *Sensors (Basel,*
688 *Switzerland)*, 20, 3516.

689 EOH, H. J., CHUNG, M. K. & KIM, S.-H. 2005. Electroencephalographic study of drowsiness in simulated
690 driving with sleep deprivation. *International Journal of Industrial Ergonomics*, 35, 307-320.

691 FENG, Y., ZHANG, S. & WU, P. 2015. Factors influencing workplace accident costs of building projects. *Safety*
692 *science*, 72, 97-104.

693 GIANNAKAKIS, G., MANOUSOS, D., SIMOS, P. & TSIKNAKIS, M. Head movements in context of speech
694 during stress induction. 2018 13th IEEE International Conference on Automatic Face & Gesture
695 Recognition (FG 2018), 2018. IEEE, 710-714.

696 GIANNAKAKIS, G., PEDIADITIS, M., MANOUSOS, D., KAZANTZAKI, E., CHIARUGI, F., SIMOS, P. G.,
697 MARIAS, K. & TSIKNAKIS, M. 2017. Stress and anxiety detection using facial cues from videos.
698 *Biomedical Signal Processing and Control*, 31, 89-101.

699 HAN, Y., JIN, R., WOOD, H. & YANG, T. 2019. Investigation of Demographic Factors in Construction Employees'
700 Safety Perceptions. *KSCE Journal of Civil Engineering*, 23, 2815-2828.

701 HAN, Y., YIN, Z., ZHANG, J., JIN, R. & YANG, T. 2020. Eye-Tracking Experimental Study Investigating the
702 Influence Factors of Construction Safety Hazard Recognition. *Journal of Construction Engineering and*
703 *Management*, 146, 04020091.

704 HART, S. G. 2006. Nasa-Task Load Index (NASA-TLX); 20 Years Later. *Proceedings of the Human Factors and*
705 *Ergonomics Society Annual Meeting*, 50, 904-908.

706 HENNI, K., MEZGHANI, N., GOUIN-VALLERAND, C., RUER, P., OUAKRIM, Y. & VALLIÈRES, É. Feature
707 selection for driving fatigue characterization and detection using visual-and signal-based sensors.
708 *Applied Informatics*, 2018. Springer, 1-15.

709 HOPSTAKEN, J. F., VAN DER LINDEN, D., BAKKER, A. B. & KOMPIER, M. A. 2015. A multifaceted
710 investigation of the link between mental fatigue and task disengagement. *Psychophysiology*, 52, 305-15.

711 HWANG, S., JEBELLI, H., CHOI, B., CHOI, M. & LEE, S. 2018. Measuring workers' emotional state during
712 construction tasks using wearable EEG. *Journal of Construction Engineering and Management*, 144,
713 04018050.

714 ILO 2022. International Labour Organization, World statistic. The enormous burden of poor working conditions.
715 *International Labour Organization*.

716 IWASAKI, M. & NOGUCHI, Y. 2016. Hiding true emotions: micro-expressions in eyes retrospectively concealed
717 by mouth movements. *Scientific Reports*, 6, 22049.

718 IZMIRLIAN, G. 2020. Strong consistency and asymptotic normality for quantities related to the Benjamini–
719 Hochberg false discovery rate procedure. *Statistics & Probability Letters*, 160, 108713.

720 JEBELLI, H., HWANG, S. & LEE, S. 2018a. EEG-based workers' stress recognition at construction sites.
721 *Automation in Construction*, 93, 315-324.

722 JEBELLI, H., HWANG, S. & LEE, S. 2018b. EEG signal-processing framework to obtain high-quality brain
723 waves from an off-the-shelf wearable EEG device. *Journal of Computing in Civil Engineering*, 32,
724 04017070.

725 JEBELLI, H., MAHDI KHALILI, M. & LEE, S. 2019. A Continuously Updated, Computationally Efficient Stress
726 Recognition Framework Using Electroencephalogram (EEG) by Applying Online Multitask Learning
727 Algorithms (OMTL). *IEEE J Biomed Health Inform*, 23, 1928-1939.

728 JEON, J. & CAI, H. 2022. Multi-class classification of construction hazards via cognitive states assessment using
729 wearable EEG. *Advanced Engineering Informatics*, 53, 101646.

730 KAUR, C., SINGH, P., BISHT, A., JOSHI, G. & AGRAWAL, S. 2022. Recent Developments in Spatio-Temporal
731 EEG Source Reconstruction Techniques. *Wireless Personal Communications*, 122, 1531-1558.

732 KE, J., DU, J. & LUO, X. 2021a. The effect of noise content and level on cognitive performance measured by
733 electroencephalography (EEG). *Automation in Construction*, 130, 103836.

734 KE, J., ZHANG, M., LUO, X. & CHEN, J. 2021b. Monitoring distraction of construction workers caused by noise
735 using a wearable Electroencephalography (EEG) device. *Automation in Construction*, 125, 103598.

736 KIMMELMAN, V., IMASHEV, A., MUKUSHEV, M. & SANDYGULOVA, A. 2020. Eyebrow position in
737 grammatical and emotional expressions in Kazakh-Russian Sign Language: A quantitative study. *PLOS*
738 *ONE*, 15, e0233731.

739 KING, D. E. 2009. Dlib-ml: A machine learning toolkit. *The Journal of Machine Learning Research*, 10, 1755-
740 1758.

741 KUSANO, H., HORIGUCHI, Y., BABA, Y. & KASHIMA, H. Stress Prediction from Head Motion. 2020 IEEE
742 7th International Conference on Data Science and Advanced Analytics (DSAA), 6-9 Oct. 2020 2020. 488-
743 495.

744 KUWAHARA, A., NISHIKAWA, K., HIRAKAWA, R., KAWANO, H. & NAKATOH, Y. 2022. Eye fatigue
745 estimation using blink detection based on Eye Aspect Ratio Mapping (EARM). *Cognitive Robotics*, 2, 50-
746 59.

747 LABOR, H. K. D. O. 2022. Summary of Occupational Safety and Health Statistics of 1st Quarter of 2022,

748 https://www.labour.gov.hk/common/osh/pdf/summary_OSH_Statistics_en.pdf (Accessed on: 12 August
749 2022).

750 LABOR, U. D. O. 2016. Commonly used statistics, Available from
751 <https://www.osha.gov/oshstats/commonstats.html>.

752 LAL, S. K. & CRAIG, A. 2002. Driver fatigue: electroencephalography and psychological assessment.
753 *Psychophysiology*, 39, 313-321.

754 LAL, S. K. & CRAIG, A. 2005. Reproducibility of the spectral components of the electroencephalogram during
755 driver fatigue. *International Journal of Psychophysiology*, 55, 137-143.

756 LEE, B. G., CHOI, B., JEBELLI, H. & LEE, S. 2021. Assessment of construction workers' perceived risk using
757 physiological data from wearable sensors: A machine learning approach. *Journal of Building Engineering*,
758 42, 102824.

759 LEE, G. & LEE, S. 2022. Feasibility of a Mobile Electroencephalogram (EEG) Sensor-Based Stress Type
760 Classification for Construction Workers. *Construction Research Congress 2022*.

761 LEE, H.-W., PENG, F.-F., LEE, X.-Y., DAI, H.-N. & ZHU, Y. Research on face detection under different lighting.
762 2018 IEEE International Conference on Applied System Invention (ICASI), 2018. IEEE, 1145-1148.

763 LI, G., HUANG, S., XU, W., JIAO, W., JIANG, Y., GAO, Z. & ZHANG, J. 2020a. The impact of mental fatigue
764 on brain activity: a comparative study both in resting state and task state using EEG. *BMC Neuroscience*,
765 21, 20.

766 LI, H., WANG, D., CHEN, J., LUO, X., LI, J. & XING, X. 2019a. Pre-service fatigue screening for construction
767 workers through wearable EEG-based signal spectral analysis. *Automation in Construction*, 106, 102851.

768 LI, J., LI, H., UMER, W., WANG, H., XING, X., ZHAO, S. & HOU, J. 2020b. Identification and classification of
769 construction equipment operators' mental fatigue using wearable eye-tracking technology. *Automation in*
770 *Construction*, 109, 103000.

771 LI, J., LI, H., WANG, H., UMER, W., FU, H. & XING, X. 2019b. Evaluating the impact of mental fatigue on
772 construction equipment operators' ability to detect hazards using wearable eye-tracking technology.
773 *Automation in Construction*, 105, 102835.

774 LI, R., CHEN, Y. V. & ZHANG, L. 2021. A method for fatigue detection based on Driver's steering wheel grip.
775 *International Journal of Industrial Ergonomics*, 82, 103083.

776 LIAO, W., ZHANG, W., ZHU, Z. & JI, Q. A real-time human stress monitoring system using dynamic Bayesian
777 network. 2005 IEEE computer society conference on computer vision and pattern recognition
778 (CVPR'05)-workshops, 2005. IEEE, 70-70.

779 LIN, L., HUANG, C., NI, X., WANG, J., ZHANG, H., LI, X. & QIAN, Z. 2015. Driver fatigue detection based
780 on eye state. *Technology and health care*, 23, S453-S463.

781 LIU, P., CHI, H.-L., LI, X. & GUO, J. 2021. Effects of dataset characteristics on the performance of fatigue
782 detection for crane operators using hybrid deep neural networks. *Automation in Construction*, 132, 103901.

783 LIU, W., ZHANG, Z., NIE, J. & FU, B. Research on the Correlation Between the Viewing Screen Layout of In-
784 Vehicle Information Terminal and Crew's Mental Workload. International Conference on Man-Machine-

785 Environment System Engineering, 2016. Springer, 341-346.

786 MA, J., LI, X., REN, Y., YANG, R. & ZHAO, Q. 2021. Landmark-Based Facial Feature Construction and Action
787 Unit Intensity Prediction. *Mathematical Problems in Engineering*, 2021, 6623239.

788 MASULLO, M., TOMA, R., PASCALE, A., RUGGIERO, G. & MAFFEI, L. Research methodology used to
789 investigate the effects of noise on overhead crane operator's performances. International Ergonomics
790 Conference, 2020. Springer, 223-231.

791 MEM 2018. "A report on the safety production situation of the national construction industry" available at:
792 https://www.mem.gov.cn/awhsy_3512/awhbgswj/201807/t20180725_247933.shtml (accessed on 14
793 August 2022).

794 NOGHABAEI, M., HAN, K. & ALBERT, A. 2021. Feasibility Study to Identify Brain Activity and Eye-Tracking
795 Features for Assessing Hazard Recognition Using Consumer-Grade Wearables in an Immersive Virtual
796 Environment. *Journal of Construction Engineering and Management*, 147, 04021104.

797 NORZALI, M., KASHIMA, M., SATO, K. & WATANABE, M. Facial Visual-Infrared Stereo Vision Fusion
798 Measurement as an Alternative for Physiological Measurement. 2014.

799 OSHA 2019. US Department of Labor, Commonly Used Statistics (Accessed on: 25 March 2022)
800 <https://www.osha.gov/data/commonstats>.

801 PALEJEV, D. & SAVOV, M. 2021. On the Convergence of the Benjamini–Hochberg Procedure. *Mathematics*, 9,
802 2154.

803 PBS 2015. "Pakistan Bureau of Statistics - Labour Force Statistics (2014-15)", Islamabad, available at:
804 https://www.pbs.gov.pk/sites/default/files/labour_force/publications/lfs2014_15/t33-pak.pdf (accessed on
805 14 August 2022).

806 PBS 2018. "Pakistan Bureau of Statistics – Labour Force Statistics (2017-18)", PBS, Islamabad, available at:
807 https://www.pbs.gov.pk/sites/default/files/labour_force/publications/lfs2017_18/Table-30_perc_R.pdf
808 (accessed on 14 August 2022).

809 PBS 2021. "Pakistan Bureau of Statistics – Labour Force Statistics (2020-21)", PBS, Islamabad, available at:
810 https://www.pbs.gov.pk/sites/default/files/labour_force/publications/lfs2020_21/tables/Table_28.pdf
811 (accessed on 14 August 2022).

812 PUSPAWARDHANI, E. H., SURYOPUTRO, M. R., SARI, A. D., KURNIA, R. D. & PURNOMO, H. 2016.
813 Mental workload analysis using NASA-TLX method between various level of work in plastic injection
814 division of manufacturing company. *Advances in safety management and human factors*. Springer.

815 RAHEEL, A., MAJID, M., ALNOWAMI, M. & ANWAR, S. M. 2020. Physiological Sensors Based Emotion
816 Recognition While Experiencing Tactile Enhanced Multimedia. *Sensors*, 20, 4037.

817 RAHEEL, A., MAJID, M. & ANWAR, S. M. 2021. DEAR-MULSEMEDIA: Dataset for emotion analysis and
818 recognition in response to multiple sensorial media. *Information Fusion*, 65, 37-49.

819 RAVAJA, N., SAARI, T., SALMINEN, M., LAARNI, J. & KALLINEN, K. 2006. Phasic Emotional Reactions to
820 Video Game Events: A Psychophysiological Investigation. *Media Psychology*, 8, 343-367.

821 SAVITZKY, A. & GOLAY, M. J. 1964. Smoothing and differentiation of data by simplified least squares

822 procedures. *Analytical chemistry*, 36, 1627-1639.

823 SHI, S.-Y., TANG, W.-Z. & WANG, Y.-Y. A review on fatigue driving detection. ITM Web of Conferences, 2017.

824 EDP Sciences, 01019.

825 SUN, Y., LIM, J., KWOK, K. & BEZERIANOS, A. 2014. Functional cortical connectivity analysis of mental

826 fatigue unmasks hemispheric asymmetry and changes in small-world networks. *Brain and cognition*, 85,

827 220-230.

828 SUNDELIN, T., LEKANDER, M., KECKLUND, G., VAN SOMEREN, E. J. W., OLSSON, A. & AXELSSON,

829 J. 2013. Cues of Fatigue: Effects of Sleep Deprivation on Facial Appearance. *Sleep*, 36, 1355-1360.

830 SWEENEY, K. T., WARD, T. E. & MCLOONE, S. F. 2012. Artifact Removal in Physiological Signals—Practices

831 and Possibilities. *IEEE Transactions on Information Technology in Biomedicine*, 16, 488-500.

832 TANG, X., ZHOU, P. & WANG, P. Real-time image-based driver fatigue detection and monitoring system for

833 monitoring driver vigilance. 2016 35th Chinese Control Conference (CCC), 27-29 July 2016 2016.

834 4188-4193.

835 TIJS, T. J. W., BROKKEN, D. & IJSSELSTEIJN, W. A. Dynamic Game Balancing by Recognizing Affect. 2008

836 Berlin, Heidelberg. Springer Berlin Heidelberg, 88-93.

837 TRAN, C.-K., TSENG, C.-D., CHANG, L. & LEE, T.-F. 2019. Face recognition under varying lighting conditions:

838 improving the recognition accuracy for local descriptors based on weber-face followed by difference of

839 Gaussians. *Journal of the Chinese Institute of Engineers*, 42, 593-601.

840 TURNER, M. & LINGARD, H. 2020. Examining the interaction between bodily pain and mental health of

841 construction workers. *Construction Management and Economics*, 38, 1009-1023.

842 TYAS, A. E., WIBAWA, A. D. & PURNOMO, M. H. Theta, Alpha and Beta Activity in the Occipital Based on

843 EEG Signals for Mental Fatigue in High School Students. 2020 International Conference on Smart

844 Technology and Applications (ICoSTA), 20-20 Feb. 2020 2020. 1-7.

845 UMER, W. 2022. Simultaneous monitoring of physical and mental stress for construction tasks using physiological

846 measures. *Journal of Building Engineering*, 46, 103777.

847 UMER, W., LI, H., YANTAO, Y., ANTWI-AFARI, M. F., ANWER, S. & LUO, X. 2020. Physical exertion

848 modeling for construction tasks using combined cardiorespiratory and thermoregulatory measures.

849 *Automation in Construction*, 112, 103079.

850 UMER, W., YU, Y. & AFARI, M. F. A. 2022. Quantifying the Effect of Mental Stress on Physical Stress for

851 Construction Tasks. *Journal of Construction Engineering and Management*, 148, 04021204.

852 WAGSTAFF, A. S. & SIGSTAD LIE, J.-A. 2011. Shift and night work and long working hours – a systematic

853 review of safety implications. *Scandinavian Journal of Work, Environment & Health*, 173-185.

854 WANG, D., CHEN, J., ZHAO, D., DAI, F., ZHENG, C. & WU, X. 2017. Monitoring workers' attention and

855 vigilance in construction activities through a wireless and wearable electroencephalography system.

856 *Automation in construction*, 82, 122-137.

857 WANG, D., LI, H. & CHEN, J. 2019. Detecting and measuring construction workers' vigilance through hybrid

858 kinematic-EEG signals. *Automation in Construction*, 100, 11-23.

- 859 WANG, M., ZHAO, Y. & LIAO, P.-C. 2022. EEG-based work experience prediction using hazard recognition.
860 *Automation in Construction*, 136, 104151.
- 861 WANG, Y., ZHAI, G., ZHOU, S., CHEN, S., MIN, X., GAO, Z. & HU, M. 2018. Eye fatigue assessment using
862 unobtrusive eye tracker. *Ieee Access*, 6, 55948-55962.
- 863 WENHUI, L., WEIHONG, Z., ZHIWEI, Z. & QIANG, J. A Real-Time Human Stress Monitoring System Using
864 Dynamic Bayesian Network. 2005 IEEE Computer Society Conference on Computer Vision and Pattern
865 Recognition (CVPR'05) - Workshops, 21-23 Sept. 2005 2005. 70-70.
- 866 XING, X., ZHONG, B., LUO, H., ROSE, T., LI, J. & ANTWI-AFARI, M. F. 2020a. Effects of physical fatigue on
867 the induction of mental fatigue of construction workers: A pilot study based on a neurophysiological
868 approach. *Automation in Construction*, 120.
- 869 XING, X., ZHONG, B., LUO, H., ROSE, T., LI, J. & ANTWI-AFARI, M. F. 2020b. Effects of physical fatigue on
870 the induction of mental fatigue of construction workers: A pilot study based on a neurophysiological
871 approach. *Automation in Construction*, 120, 103381.
- 872 ZARGARI MARANDI, R., MADELEINE, P., OMLAND, Ø., VUILLERME, N. & SAMANI, A. 2018. Eye
873 movement characteristics reflected fatigue development in both young and elderly individuals. *Scientific*
874 *Reports*, 8, 13148.
- 875 ZHANG, Z. & ZHANG, J. 2010. A new real-time eye tracking based on nonlinear unscented Kalman filter for
876 monitoring driver fatigue. *Journal of Control Theory and Applications*, 8, 181-188.
- 877 ZHAO, C., ZHAO, M., LIU, J. & ZHENG, C. 2012. Electroencephalogram and electrocardiograph assessment of
878 mental fatigue in a driving simulator. *Accident Analysis & Prevention*, 45, 83-90.
- 879